



**INSTITUTO POTOSINO DE INVESTIGACIÓN
CIENTÍFICA Y TECNOLÓGICA, A.C.**

POSGRADO EN CIENCIAS EN BIOLOGIA MOLECULAR

**Heteromeric channels with different phenotypes
are generated when coexpressing two P2X2
receptor isoforms**

Tesis que presenta

Josue Obed Jaramillo Polanco

Para obtener el grado de

Doctor en Ciencias en Biología Molecular

Director de la Tesis:

Dr. Carlos Barajas López

San Luis Potosí, S.L.P., Septiembre de 2016



Constancia de aprobación de la tesis

La tesis “**Heteromeric channels with different phenotypes are generated when coexpressing two P2X2 receptor isoforms**” presentada para obtener el Grado de Doctor(a) en Ciencias en Biología Molecular fue elaborada por **Josue Obed Jaramillo Polanco** y aprobada el **5 de agosto de 2016** por los suscritos, designados por el Colegio de Profesores de la División de Biología Molecular del Instituto Potosino de Investigación Científica y Tecnológica, A.C.

Dr. Carlos Barajas López
(Director de la tesis)

Dr. Juan Francisco Jiménez Bremont
(Asesor de la tesis)

Dra. Marcela Miranda Morales
(Asesor de la tesis)

Dr. Sergio Ramón Sánchez Armass
Acuña
(Asesor de la tesis)

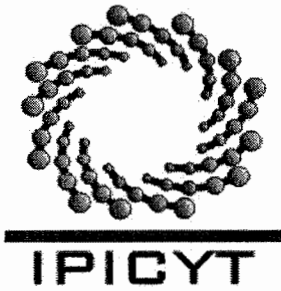
Dr. Rogelio Arellano Ostoa
(Asesor de la tesis)



Créditos Institucionales

Esta tesis fue elaborada en el Laboratorio de Neurobiología de la División de Biología Molecular del Instituto Potosino de Investigación Científica y Tecnológica, A.C., bajo la dirección del Dr. Carlos Barajas López.

Durante la realización del trabajo el autor recibió una beca académica del Consejo Nacional de Ciencia y Tecnología (36691) y del Instituto Potosino de Investigación Científica y Tecnológica, A. C.



Instituto Potosino de Investigación Científica y Tecnológica, A.C.

Acta de Examen de Grado

El Secretario Académico del Instituto Potosino de Investigación Científica y Tecnológica, A.C., certifica que en el Acta 087 del Libro Primero de Actas de Exámenes de Grado del Programa de Doctorado en Ciencias en Biología Molecular está asentado lo siguiente:

En la ciudad de San Luis Potosí a los 14 días del mes de septiembre del año 2016, se reunió a las 16:00 horas en las instalaciones del Instituto Potosino de Investigación Científica y Tecnológica, A.C., el Jurado integrado por:

Dr. Juan Francisco Jiménez Bremont	Presidente	IPICYT
Dr. Carlos Barajas López	Secretario	IPICYT
Dra. Marcela Miranda Morales	Sinodal externo	UASLP
Dr. Sergio Ramón Sánchez Armass Acuña	Sinodal externo	UASLP

a fin de efectuar el examen, que para obtener el Grado de:

DOCTOR EN CIENCIAS EN BIOLOGÍA MOLECULAR

sustentó el C.

Josué Obed Jaramillo Polanco

sobre la Tesis intitulada:

Heteromeric channels with different phenotypes are generated when coexpressing two P2X2 receptor isoforms

que se desarrolló bajo la dirección de


Dr. Carlos Barajas López

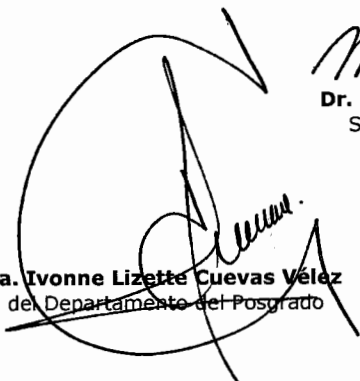
El Jurado, después de deliberar, determinó

APROBARLO

Dándose por terminado el acto a las 18:23 horas, procediendo a la firma del Acta los integrantes del Jurado. Dando fe el Secretario Académico del Instituto.

A petición del interesado y para los fines que al mismo convengan, se extiende el presente documento en la ciudad de San Luis Potosí, S.L.P., México, a los 14 días del mes de septiembre de 2016.


Dr. Marcial Bonilla Marín
Secretario Académico


Mtra. Ivonne Lizette Cuevas Vélez
Jefa del Departamento del Posgrado

Dedicatorias

A mis padres, Juan Jaramillo Vergara y Ma Salomé Polanco Mellín.

A Cintya del Refugio López López que me acompaña y motiva.

Agradecimientos

Al Dr. Carlos Barajas López por la oportunidad de trabajar en su laboratorio, su asesoría, correcciones y el apoyo que me brindó.

A los Doctores miembros de mi comité tutorial (Juan Francisco Jiménez Bremont, Marcela Miranda Morales, Sergio Sánchez Armass Acuña y Rogelio Arellano Ostoa) por sus observaciones y sugerencias, siempre en la mejora del proyecto.

A Rosa Espinosa Luna por todo el apoyo dentro y fuera del laboratorio, las enseñanzas y los consejos.

Dra. Andrómeda Liñán, Dr. Raúl Loera, Dra. María Guadalupe Nieto, Cintya del Refugio López, Karen Zarahi Gómez, Jessica Rodríguez, gracias por permitirme colaborar con ustedes.

A la Sra. Rosa Cruz por toda la atención y apoyo en el laboratorio y con las ranas.

A mis compañeros del Laboratorio de Neurobiología, así como a los de Biología Molecular por la amistad y los buenos momentos mientras aprendíamos.

A mi Familia por todo su apoyo, siempre.

Content

Constancia de aprobación de la tesis	ii
Créditos institucionales	iii
Acta de examen	iv
Dedicatorias	v
Agradecimientos	vi
Content	vii
List of tables	ix
List of figures	x
List of appendixes	xi
Abbreviations	xii
Glossary	xiii
Resumen	xiv
Abstract	xv
1. INTRODUCTION	1
1.1. Synaptic transmission	1
1.2. Chemical synaptic transmission	3
1.2.1. Neurotransmitters	4
1.2.2. G protein-coupled receptors	5
1.2.3. Ligand-gated ion channels	6
1.3. Purinergic signalling	7
1.3.1. P2Y receptors	8
1.3.2. P2X receptors	8
2. BACKGROUND	10
3. THE RATIONALE BEHIND THIS STUDY	13
4. HYPOTHESIS	14
5. GENERAL OBJECTIVE	15
6. MATERIALS AND METHODS	16
6.1. Genomic sequence analysis of P2Xreceptors	16
6.2. Cloning of P2X2 receptors	16
6.3. Preparation of <i>Xenopus laevis</i> oocytes	17
6.4. Electrophysiological recordings	18
6.5. Drugs application	18
6.6. Solutions and reagents	19

6.7. Data analysis	19
7. RESULTS	21
7.1. General properties of homomeric channels	21
7.2. General properties of channels formed in coexpression experiments	23
7.3. Current kinetics	25
7.4. ATP threshold and Hill coefficients	29
7.5. PPADS inhibitory effects	31
8. DISCUSSION	33
9. CONCLUSION	40
10. REFERENCES	41
APPENDIX A	47
APPENDIX B	49
APPENDIX C	51

List of tables

1. Properties of P2X2-1a and P2X2-2b receptors expressed in *Xenopus laevis* 12
2. Summary of homomeric and coexpressed channel properties. 21
3. Desensitization kinetics parameters can predict when a homomeric channel contributes 10% to the maximal current 25

List of figures

1. The two modalities of synaptic transmission.	2
2. Structure and function of P2X receptors.	9
3. Kinetics and ATP sensitivities of P2X2-1 and P2X2-2.	12
4. Homomeric channels have different kinetics and sensitivity to ATP and BzATP.	22
5. Channels formed by P2X2-1a/P2X2-2bm coexpression can be classified into at least two different groups.	24
6. Current kinetics indicates that P2X2-1a like or P2X2-2bm like currents are not mediated by a significant expression of homomeric channels.	26
7. ATP threshold concentration for these currents suggests that a P2X2-1a homomeric channels does not significantly contribute to P2X2-1a like currents but their Hill coefficient suggest that P2X2-1a and P2X2bm subunits are required to activate P2X2-1a like P2X2-2bm like currents.	30
8. PPADS sensitivity of heteromeric channels is the same and similar to low sensitivity homomeric (P2X2-2bm) receptors.	32
9. Activation of P2X2 channels by occupancy of two ATP binding sites.	37

List of appendixes

- | | |
|---|----|
| A. Heteromeric channels with different phenotypes are generated when coexpressing two P2X2 receptor isoforms. | 48 |
| B. Retention of a new-defined intron changes pharmacology and kinetics of the full-length P2X2 receptor found in myenteric neurons of the guinea pig. | 50 |
| C. Genomic organization of purinergic P2X receptors. | 52 |

Abbreviations

aa	Amino acids
α,β-meATP	α,β -methylene ATP
ACh.	Acetylcholine
ATP	Adenosine-5'-triphosphate
BzATP	2'-3'-O-(4-benzoylbenzoyl)-ATP
cDNA	Complementary DNA
EC₅₀ (IC₅₀)	Half maximal effective (or inhibitory) concentration
GABA	γ -aminobutyric acid, 5-hydroxytryptamine
GABA_A, GABA_B	Receptors GABA _A
GABA_B	Receptors GABA _B
GPCRs	G-protein Coupled Receptors
nAChR	Nicotinic Acetyl Choline Receptors
I_{ATP}	ATP-induced currents
NCBI	National Center for Biotechnology Information
ORF	Open Reading Frame
PCR	Polymerase Chain Reaction
PPADS	Pyridoxalphosphate-6-azophenyl-2',4'-disulphonic acid
SNAP	Soluble NSF Attachment Protein
SNARE	SNAP Receptor
UTR	Untranslated region
VGCC	Voltage-gated cation channel
5HT3R	Ionotropic 5-hydroxytryptamine receptor

Glossary

Agonist. Is a chemical that binds and activates a given receptor, triggering a response in the cell.

Alternative splicing. A mechanism in which different combinations of exons are joined together during the final stages of transcription so that more than one messenger RNA is produced from a single gene

Antagonist. Is a receptor ligand that does not provoke a biological response by itself but blocks or dampens a cell response induced by an agonist.

Desensitization. Reduction of the cell response induced by an agonist when this is continuously or repetitively administered.

EC₅₀ and IC₅₀. Refers to the concentration of agonist or antagonist that induces a response halfway between the baseline and the maximum after some specified exposure time.

Heterologous expression. The expression of a gene or part of a gene in a host organism, which does not naturally have this gene or gene fragment.

Hill coefficient. Is a measure of cooperativity during the binding process of the agonists and antagonists to the receptor binding sites. A coefficient of 1 indicates completely independent binding, regardless of how many additional ligands are already bound. Numbers greater than unity indicate positive cooperativity, while less than unity negative cooperativity.

Isoforms. Functionally similar proteins that have a similar but not an identical amino acid sequence

P2X receptors. Receptor membrane proteins activated by ATP, which include an ion channel.

Splicing variant. Active mRNA that results from cutting and resealing or a RNA transcript by precise breakage of phosphodiester bonds at the 5' and 3' splice sites (exon-intron junction)

Stoichiometry. Quantitative relationship of the various subunits that conform a given protein, e.g. ion channel.

Synaptic vesicle. Is a small secretory vesicle that contains a neurotransmitter, is found inside an axon near the presynaptic membrane, and releases its contents into the synaptic cleft

Synaptic cleft. The space between neurons at a nerve synapse across which a nerve impulse is transmitted by a neurotransmitter.

Two-electrode voltage clamp technique. Is a common electrophysiological technique that allows ion flow across the cell membrane to be measured as an electric current while the transmembrane potential is held constant with a feedback amplifier. Ion channels expressed in *Xenopus* oocytes can be studied using the two-microelectrode voltage clamp technique.

Resumen

Heteromeric channels with different phenotypes are generated when coexpressing two P2X2 receptor isoforms

Para determinar si al coexpresar dos isoformas del receptor P2X2 en ovocitos de *Xenopus laevis* se forman canales heteroméricos con diferente estequiometría. Tomando ventaja de una mutante (P2X2-2bm) debido a que tiene una menor sensibilidad al ATP que el receptor P2X2-2b (*wild type*), y a su vez incrementa las diferencias entre esta y la variante P2X2-1a. Los canales P2X son triméricos con tres sitios de unión al agonista, dos posibles combinaciones pueden dar lugar a los canales heteroméricos: i) 2(P2X2-1a) +1(P2X2-2bm); o ii) 1(P2X2-1a) +2(P2X2-2bm). Debido a que la apertura de los canales P2X se da por la unión de dos moléculas del ATP, se esperaría diferente sensibilidad al ATP entre estos heterómeros. En apoyo a esta hipótesis, la coexpresión de las dos isoformas de receptor P2X2 resultó en dos poblaciones de ovocitos con sensibilidad al ATP y coeficientes de Hill diferentes. Una población (P2X2-1a like), fue similar a los ovocitos en que solo se expresaron canales P2X2-1a, mientras la otra (P2X2-2bm like) fue similar a cuando solo se expresaron canales P2X2-2bm. Sin embargo, el análisis de sus cinéticas, descarta la expresión de canales homoméricos. Los datos también indican que, la heteromerización de los canales, provoca cambios en la cinética de desensibilización. En conclusión, cuando las isoformas de P2X2 son coexpresadas, los ovocitos expresan principalmente una de las dos estequiometrías de canales heteroméricos.

PALABRAS CLAVE: Receptores P2X, activación de receptores P2X, estequiometría de receptores P2X, variantes de *splicing*, expresión heteróloga, inhibidor PPADS.

Abstract

Heteromeric channels with different phenotypes are generated when coexpressing two P2X2 receptor isoforms

To investigate if channels with different stoichiometry are formed from two P2X2 receptor splice variants during their co-expression in *Xenopus laevis* oocytes. We used a mutant (P2X2-2bm) because it has a lower ATP sensitivity than the wild type receptor. P2X channels are trimeric proteins with three agonist binding sites; therefore, only two homomeric and two heteromeric stoichiometries are possible, the heteromeric channels might be formed by: **i)** 2(P2X2-1a) +1(P2X2-2bm); or **ii)** 1(P2X2-1a) +2(P2X2-2bm). Because P2X2 channels open when two binding sites are occupied, these stoichiometries are expected to have different sensitivities to ATP. In agreement with this, coexpressing both P2X2 isoforms, two oocyte populations were distinguished based on their channel sensitivities to ATP and Hill coefficients. For the first population (P2X2-1a like), such parameters were not different than those of homomeric P2X2-1a channels, and for the second population (P2X2-2bm like), these parameters were also not different than for homomeric P2X2-2bm channels. Kinetics analysis indicates that heteromeric channel expression is occurring, and homomeric channel expression is not responsible for such differences. Our data indicate that oocytes expressed heteromeric channels with mainly one (of the two possible) stoichiometry when P2X2-1a and P2X2-2bm subunits are coexpressed, and the expression of homomeric channels is also not detectable.

KEY WORDS: P2X receptors, P2X receptor activation, P2X receptor stoichiometry, splicing variants, heterologous expression, PPADS binding.

INTRODUCTION

1.1. Synaptic transmission

Neurons communicate with other neurons or effectors cells at anatomically identifiable cellular regions called synapsis. Such communication is known as synaptic transmission, and two modalities are recognized, chemical and electrical (Fig. 1). At chemical synapses, information is transferred through the exocytotic release of a neurotransmitter from one presynaptic neuron at the synaptic cleft and detection of the neurotransmitter by a postsynaptic adjacent cell; whereas in electrical synapses, the cytoplasm of adjacent cells is directly connected by clusters of intercellular channels called gap junctions, resulting in a low electrical resistance communication (Pereda, 2014).

Structurally, the neuron is made up of a cell body or soma, a single axon, and dendrites. The cell body contains the nucleus and cytoplasmic organelles with a large amount of rough endoplasmic reticulum. The axon is the longest cell process, capable of transmitting nerve impulses and/or releasing exocytic vesicles contained in the axon terminals. The dendrites are shorter and more branched than the axon, the number of dendrites defines the kind of neuron. If there is no dendrite, it is a unipolar neuron; with one dendrite, it is a bipolar neuron; if there is more than one dendrite, it is a multipolar neuron. Pseudounipolar neurons have just a single process leaves the soma and then bifurcates (Craig *et al.*, 1994; Tahirovic *et al.*, 2009).

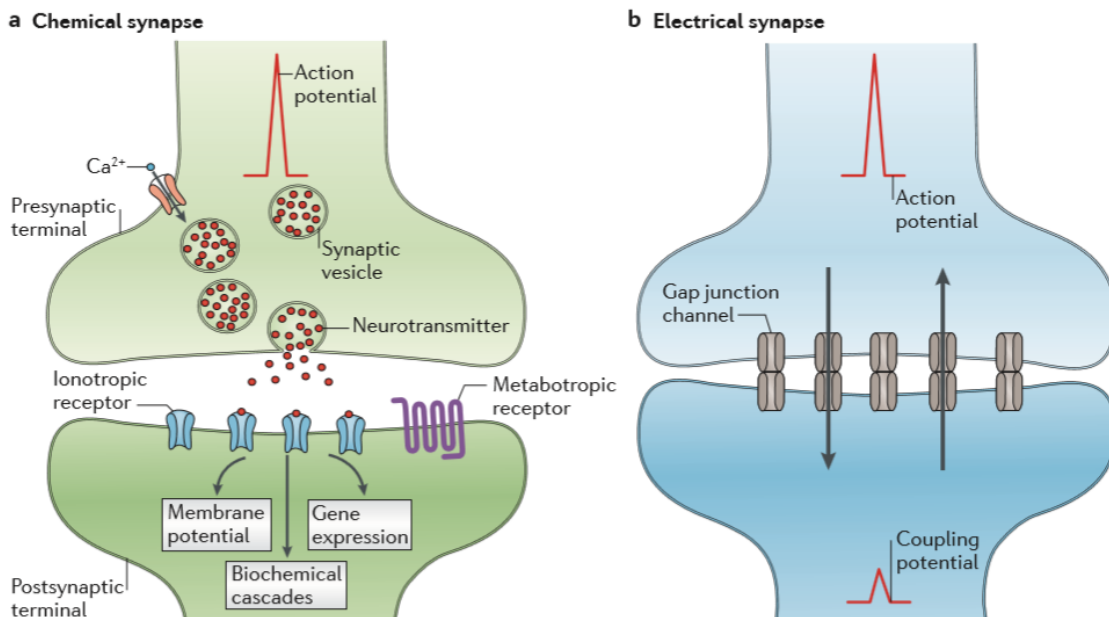


Figure 1: The two modalities of synaptic transmission. **a)** Simplified diagram of chemical synapses. Depolarization of the presynaptic terminal by the arrival of an action potential evokes the neurotransmitter release, which leads to the activation of voltage-gated calcium channels (VGCCs). Then, in the postsynaptic terminal, the ionotropic and metabotropic receptors are capable of detecting and translating the presynaptic message (neurotransmitters) into various postsynaptic events (changes in resting membrane potential, biochemical cascades activation and regulation of gene expression). **b)** Simplified diagram of electrical synapses. Clusters of gap junctions that connect the interior of two adjacent cells and thereby, directly enable the bidirectional passage of ionic currents (arrows), as well as, intracellular messengers and small metabolites (modified from Pereda, 2014)

Although, synapses for both forms of transmission can be found between different neuronal sites (dendrites, soma, and axons), chemical transmission normally occurs between synaptic terminals from axons and the dendrite or soma of a postsynaptic neuron, or effector cell (muscle fibre or gland cell). The cell-cell communication system is not unique to the nervous system, for example, the transfer of information between cells of the immune system, shares some

characteristics of neuronal chemical and electrical synapses, which has led to the adoption of the common term “immune synapse” to describe the close cell-cell contacts (Dustin, 2012).

1.2. Chemical synaptic transmission

The chemical synaptic transmission, involving the exocytotic release of neurotransmitter from presynaptic cells, produces depolarizing or hyperpolarizing currents on the postsynaptic cell, resulting in postsynaptic potentials (excitatory or inhibitory, respectively), that are fast if they are mediated by ligand-gated ion channels (LGICs), or slow if they are mediated by G protein-coupled receptors (GPCRs)(Galligan, 2002a; Galligan, 2002b; Greengard, 2001).

In the presynaptic terminal, the exocytosis of neurotransmitters is triggered by the influx of Ca^{2+} through voltage-gated channels. A large number of proteins, including a calcium-responsive trigger protein known as synaptotagmin, are important in regulating vesicle exocytosis. The rise in Ca^{2+} concentration within the presynaptic terminal causes synaptic vesicles to fuse with the presynaptic plasma membrane and release their contents into the synaptic cleft. This process requires the interaction of different proteins, some of these, are known as SNAREs (soluble NSF-attachment protein receptors), are small membrane-anchored proteins. Specific SNAREs are found on synaptic vesicles (synaptobrevin or VAMP) and the presynaptic plasma membrane (syntaxin, and SNAP-25). Additional sets of proteins are responsible for endocytosis and regeneration of synaptic vesicles (Landis, 1988; Südhof *et al.*, 2011).

The postsynaptic side contains clusters of neurotransmitter receptors and ion channels embedded in a protein network comprised of anchoring and scaffolding molecules, signaling enzymes, cytoskeletal components, as well as other membrane proteins. Altogether, receive the neurotransmitter signal released from the presynaptic terminal and transduce it into electrical and biochemical changes in the postsynaptic cell (Südhof, 2004).

1.2.1. Neurotransmitters

A large number of different chemical messengers are released in the synapsis through exocytosis, allowing tremendous diversity in chemical signaling between neurons. The neurotransmitters can be separated into two broad categories based on size, neuropeptides, and small-molecule neurotransmitters. Neuropeptides are transmitter molecules composed of more than three amino acids, they are grouped based on their sequence (e.g. brain/gut peptides, opioid peptides). The small-molecule neurotransmitters are much smaller than neuropeptides, within this category are the individual amino acids (e.g. glutamate and GABA) as well as transmitters of different molecular origin (e.g. acetylcholine, serotonin, histamine, and ATP)(Goyal *et al.*, 2013; Kandel *et al.*, 2000).

There are molecules considered as unconventional neurotransmitters, although they involved in intercellular signaling, and their release from neurons is regulated by Ca^{2+} , they are not stored in synaptic vesicles and are not released from presynaptic terminals via exocytotic mechanisms (e.g. endocannabinoids and nitric oxide)(Boyd, 2006; Goyal *et al.*, 2013; Jaffrey *et al.*, 1995; Kandel *et al.*, 2000).

There are two major classes of receptors through which neurotransmitters evoke postsynaptic electrical or biochemical responses: LGICs in which the receptor molecule is also an ion channel; and GPCRs in which the receptor and ion channel are separate molecules (Galligan, 2002a; Greengard, 2001).

1.2.2. G protein-coupled receptors

Also known as metabotropic receptors, this because the movement of ions derived from the activation of these receptors depends on one or more metabolic steps to activate ion channels, these receptors do not have ion channels as part of their structure. GPCRs are proteins with an extracellular domain that contains a neurotransmitter binding site, seven membrane-spanning domains, and an intracellular domain that binds to G proteins. Then, neurotransmitter binding to metabotropic receptors activates G-proteins, which in turn interacts directly with ion channels or bind to other effector proteins, such as enzymes, that make intracellular messengers that open or close ion channels (Foord *et al.*, 2005; Lagerstrom *et al.*, 2008).

GPCRs may promote excitatory or inhibitory synaptic transmission through direct interaction of the G protein with ion channels or through the side effect of second messengers. However, both modes are consistent with the nature of the neurotransmitters and receptors. Receptors activated by acetylcholine (mACh) or glutamate (mGlu) trigger an excitatory effect, whereas the receptors activated by GABA (GABA_B) trigger an inhibitory effect (Greengard, 2001).

1.2.3. Ligand-gated ion channels

LGICs are membrane proteins that form a pore that allows the regulated flow of selected ions across the plasma membrane. The channels are gated by the union of a neurotransmitter which triggers a conformational change in the channel resulting in the conducting (open) state. These receptors mediate fast synaptic transmission, on a millisecond time scale, however, the expression of some LGICs is not exclusive to excitable cells, suggesting additional functions (Connolly *et al.*, 2004; Galligan, 2002a).

The LGICs comprise the excitatory (cation-selective channels), among these, those activated by acetylcholine (nACh), serotonin (5-HT₃), glutamate (NMDA and AMPA) and ATP (P2X) receptors; and the inhibitory (anion-selective channels), among these, those activated by GABA (GABA_A) and glycine (GlyR) receptors (Barnes *et al.*, 2009; Jarvis *et al.*, 2009; Lodge, 2009; Lynch, 2009; Millar *et al.*, 2009; Olsen *et al.*, 2009)

The nACh, 5-HT₃, GABA_A and glycine receptors (and an additional zinc-activated channel) are pentameric channels, also known as Cys-loop receptors due to the presence of an extracellular loop of residues formed by a disulfide bond. The ionotropic glutamate receptors are tetrameric channels, and the P2X receptors are trimeric channels. Multiple genes encoding subunits of different type of LGICs, furthermore, most of these receptors are heteromultimeric, this results in different combinations of subunits leading to a wide range of receptors with different pharmacological and biophysical properties and varying expression patterns in the nervous system and other tissues (Brady *et al.*, 2001; Conroy *et al.*, 1995; Galligan, 2002a; Saul *et al.*, 2013).

1.3. Purinergic signalling

The concept of purinergic transmission, suggesting the purines like a neurotransmitter was proposed by Burnstock in 1972. 20 years later, was cloned the first P2 receptor (Webb *et al.*, 1993). Purinergic signalling is not only involved in neuronal signalling, but also in many non-neuronal regulatory processes that include exocrine and endocrine secretion, immune responses, inflammation, pain, platelet aggregation, and endothelial-mediated vasodilatation. Cytoplasmatic ATP levels reach millimolar concentrations, and it is now recognized that damaged cells and healthy cells can release a considerable amount of ATP into the extracellular environment, where it can work like a ligand of purinergic receptors (Junger, 2011; Khakh *et al.*, 2006).

Neurons may contain concentrations up to 100 mM ATP in synaptic vesicles, from where it can be released, sometimes along with other neurotransmitters by exocytosis after a previous action potential, or in response to cellular injury or death. ATP is the molecule mostly co-released from synaptic vesicles, evidence showing that ATP is a cotransmitter with ACh, noradrenaline, glutamate, GABA and dopamine in different subpopulations of neurons in the central and peripheral nervous systems (Burnstock, 1976a; Burnstock, 2009).

Extracellular ATP is rapidly hydrolyzed by ecto-ATPases and ectonucleotidases. The metabolites (principally adenosine) obtained from this hydrolysis are also important mediators in cell signalling. ATP act on P2 receptors and adenosine act on P1 receptors. P1 are GPCRs commonly referred to as adenosine receptors (A1R, A2AR, A2BR, y A3R) (Ralevic *et al.*, 1998). ATP, ADP,

UTP and UDP act at P2 receptors, which are either LGICs (P2X) or GPCRs (P2Y) receptors (Burnstock, 1976b; Burnstock, 2006).

1.3.1. P2Y receptors

P2Y receptors are GPCRs activated by low concentrations of ATP (from nM to low μ M range). In mammals, there are at least eight genes encoding subtypes of P2Y receptor. Some P2Y receptors principally use Gq/G11 that activates the phospholipase C/inositol triphosphate endoplasmic reticulum Ca^{2+} -release pathway. Others P2Y receptors, almost exclusively, couple to Gi/o, which inhibits adenylyl cyclase and modulates ion channels. Thus, ATP binding to P2Y receptors triggers second-messenger cascades that amplify and prolong the signal over seconds. The characteristics of P2Y and P1 receptors make them appropriate for a long-lasting modulatory function because they can detect lower ATP concentrations over greater distances from the site of release (Erb *et al.*, 2012; Weisman *et al.*, 2012).

1.3.2. P2X receptors

P2X receptors are ligand-gated cation channels activated by extracellular ATP. Seven (P2X1-7) subunits, each codified by a different gene, are present in mammalian species and homomeric and heteromeric channels are constituted by trimers of P2X subunits. Subunits have two membrane-spanning domains, an extracellular domain, and intracellular N and C termini. ATP binds to the extracellular domain between the interface of two subunits and, therefore, there are three binding sites per channel (Fig. 2) (Hattori *et al.*, 2012; Kawate *et al.*, 2009;

Marquez-Klaka *et al.*, 2007; North, 2002; Torres *et al.*, 1999; Wilkinson *et al.*, 2006). The P2X subunits are different on size, being the portion C termini the most variable. This portion C termini has been related to the regulation of the channel and interactions with other ligand-activated receptors and structural proteins (Boue-Grabot *et al.*, 2003; Guimaraes, 2008; Kim *et al.*, 2001; Koshimizu *et al.*, 1999; Koshimizu *et al.*, 2006).

Splicing variants have been described for the different subunits, these are expressed in specific tissues or under specified conditions (North, 2002). Some of these variants have different pharmacological and kinetic properties compared to canonical channels, some of these lose the ability to interact with proteins or form functional channels. Not all variants have been characterized.

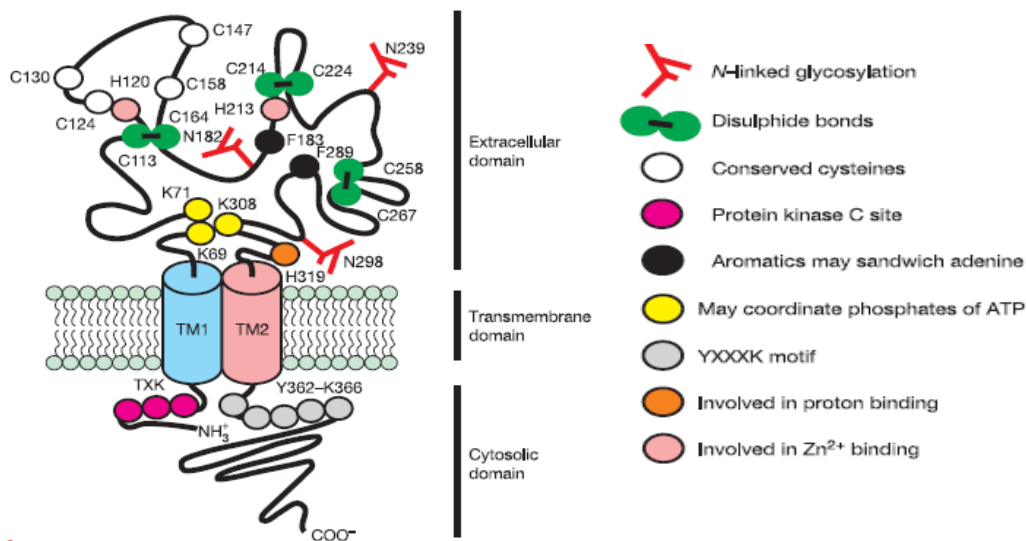


Figure 2. Structure and function of P2X receptors. Topology and key features of P2X receptor subunits. The numbers are amino acids for rat P2X2 receptors. (Khakh *et al.*, 2006)

2. BACKGROUND

P2X heteromeric complexes have been shown by coimmunoprecipitation tests, also the inability to form homotrimers of P2X6 and to form heterotrimers of P2X7 (Torres *et al.*, 1999). Heteromeric channels are known to maintain some pharmacological and biophysical properties of the participating subunits (Aschrafi *et al.*, 2004; King *et al.*, 2000; Le *et al.*, 1998; Lewis *et al.*, 1995; Nicke *et al.*, 2005; Torres *et al.*, 1999; Torres *et al.*, 1998). The heteromeric receptor P2X2/3 is one of the best characterized, which exhibits a similar rank order of agonist potency than P2X3 homomeric channels, including its sensitivity to α,β -meATP, but they are distinguished from P2X3 homomeric channels by their slower desensitization kinetics (Hausmann *et al.*, 2012; Jiang *et al.*, 2003; Lewis *et al.*, 1995; Stelmashenko *et al.*, 2012). Such experiments indicate that fewer than three binding sites need to be occupied to elicit channel opening. Additional studies, using heterologous coexpression of P2X2 and P2X3 or P2X6 receptors, have provided strong evidence that the quaternary trimeric structure would have stoichiometries of one P2X2 and two P2X3 subunits (P2X2/3[1:2]), and two P2X2 and one P2X6 subunit (P2X2/6[2:1]) (Hausmann *et al.*, 2012; Wilkinson *et al.*, 2006), which for a while were the only reported stoichiometries for heteromeric P2X receptors. However, a recent study (Kowalski *et al.*, 2015), described experimental evidence indicating that the availability of P2X2 and P2X3 subunits determined the stoichiometry of heterotrimeric P2X2/3 receptors and the other

possible stoichiometry (P2X2/3[2:1]) can also be assembled when different ratios of these pairs of receptors are co-expressed.

We have reported the properties of two recombinant isoforms of the P2X2 receptor (P2X2-1a (GenBank Accession # FJ641871.1) and P2X2-2b (GenBank accession # FJ641872.1) from guinea pig myenteric neurons, which have different kinetics and pharmacological properties (Fig. 3 and Tab. 1) (Liñan-Rico *et al.*, 2012). In the present work we co-expressed the P2X2 splice variant P2X2-1a and a version of the P2X2-2b with two mutations (named here P2X2-2bm); one in the amino terminal (E26G) and another in the extracellular region (L185Q); mutations that decrease ATP sensitivity, about 10 folds, and increase 3-5 times the desensitization kinetics (when it was expressed and characterized), which helped us to distinguish both P2X2 isoforms in the present study. Co-expression experiments show that different oocytes expressed receptors with two pharmacological profiles, one similar to P2X2-1a (P2X2-1a like) and the other to P2X2-2bm (P2X2-2bm like). In addition, P2X2-1a like and P2X2-2bm like receptors showed the same desensitization kinetics, which was significantly different to that of homomeric P2X2-1a and P2X2-2bm individual channels, and to that of the predicted desensitization for various combinations of these homomeric channels. Altogether, our data indicate that the two possible heteromeric stoichiometries can be expressed when P2X2-1a and P2X2-2bm receptors are co-expressed.

Table 1. Properties of P2X2-1a and P2X2-2b receptors expressed in *Xenopus laevis*

Receptor	Tau of desensitization (seconds)	Agonists EC ₅₀ (μM)			Antagonists IC ₅₀ (μM)	
		ATP	BzATP	α,β-me ATP	Suramin	PPADS
P2X2-1a	τ ₁ = 300±84	5±0.6 ¹ n=15	4±2 n=5	>100 n=4	0.4±0.2 n=4 486±120 ² n=3	0.8±0.2 ³ n=5
P2X2-2b	τ ₁ = 6±0.4 τ ₂ = 75±9	18±2 ¹ n=9	>100 n=6	>100 n=4	2.03±37 ² n=4	2.4±0.5 ³ n=4

Pairs of superscript numbers indicate data that were compared and were found to be statistically different ($P \leq 0.05$). (Liñan-Rico *et al.*, 2012)

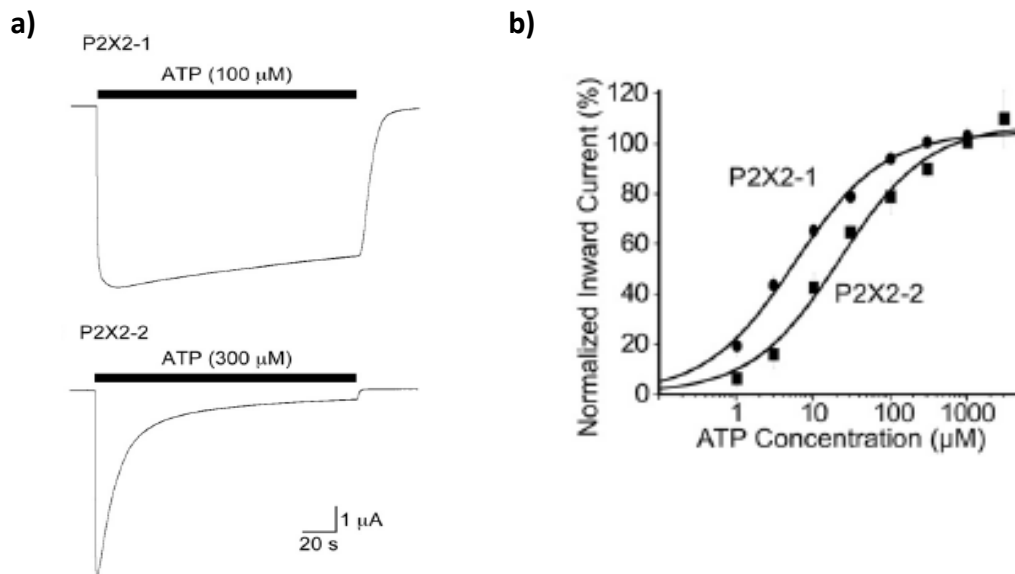


Figure 3: Kinetics and ATP sensitivities of P2X2-1 and P2X2-2. a) Representative traces of ATP induced-currents recorded from *Xenopus laevis* oocytes expressing P2X2-1 (P2X2-1a) or P2X2-2 (P2X2-2b). Horizontal bars above traces indicate the ATP application, at equipotent concentrations. b) Concentration-response curves for ATP to activate membrane currents mediated by P2X2-1 or P2X2-2 receptors. Vertical lines associated with symbols are S.E.M of relative currents. (Liñan-Rico *et al.*, 2012)

3. THE RATIONALE BEHIND THIS STUDY

P2X channels are trimeric receptors with three agonist binding sites; therefore, only two homomeric and two heteromeric stoichiometries are possible when two different P2X subunits are coexpressed, the heteromeric channels might be formed by: **i)** 2(P2X type 1) +1(P2X type 2); or **ii)** 1(P2X type 1) +2(P2X type 2).

It is known that reported heteromeric channels possess pharmacological properties that resemble the subunits that conform the channel. However, these properties are associated with one of the two possible stoichiometries.

Although heterologous coexpression and co-immunoprecipitation assays have shown the formation of two possible heteromeric stoichiometries, there is no clear evidence showing the electrophysiological properties of both heteromeric stoichiometries when two different P2X subunits are coexpressed.

The problem for not being able to demonstrate the functionality of the two possible heteromeric stoichiometries may be because these works are based on the selective activation of the subunits that make up the heteromeric, but one of the subunits is unable to respond to the agonist.

4. HYPOTHESIS

Because P2X channels are composed of three subunits, besides to the possible formation of homomeric channels, two stoichiometries of heteromeric channels are possible when P2X2-1a and P2X2-2bm are coexpressed, which might be formed by: **i)** 2(P2X2-1a) +1(P2X2-2bm); or **ii)** 1(P2X2-1a) +2(P2X2-2bm). Since P2X channels open when two subunits are activated by ATP, and P2X2-1a and P2X2-2bm have different ATP sensitivity; hence, these two putative heteromeric stoichiometries would be expected to have different ATP sensitivity.

5. GENERAL OBJECTIVE

To investigate if heteromeric channels with different stoichiometry are formed and can be differentiated when P2X2 receptor isoforms are heterologously co-expressed.

Specific aims

- Using the technique of two-electrode voltage clamp, characterize the individual expression and co-expression of P2X2-1a and P2X2-2bm receptors.
- To differentiate oocytes expressing alone or together the isoforms P2X2-1a and P2X2-2bm.
- To identify possible heteromeric channels between oocytes co-expressing the isoforms P2X2-1a and P2X2-2bm.

6. MATERIALS Y METHODS

6.1. Genomic sequence analysis of P2X receptors

Genomic and cDNA sequences encoding P2X2 receptors were obtained from the NCBI (<http://www.ncbi.nlm.nih.gov>) and Ensembl database (<http://www.ensembl.org>). Exon-intron structure of P2x2 gene was derived from the aligned cDNA/genomic sequence or obtained directly from NCBI.

6.2. Cloning of P2X2 receptor

Tissue extracted from the small intestine of Guinea Pig was triturated in a mortar with liquid nitrogen. The RNAqueous RNA isolation kit (Life Technologies, Texas, USA) was used to obtain total RNA according to the manufacturer's protocol. First strand cDNA were synthesized using Superscript reverse transcriptase II (Life Technologies, Texas, USA) in the presence of oligo (dT)₁₈ for 1.5 h at 42 °C. PCR was performed using specific guinea pig P2X2 primers designed at the 5' and 3' UTRs regions to amplify the entire coding sequence (P2X2 sense 5'-GTTCTGGGCACCATGGCTGC-3' and P2X2 antisense 5'-TCCTGTCTGCAGACCTGGCGT-3'). PCR reaction was done using Platinum Pfx Taq DNA Polymerase (Life Technologies, Texas, USA), conditions were as follows: initial denaturation for 2 min at 95 °C, then 40 amplification rounds of denaturation for 15 s at 95 °C, alignment for 20 s at 60 °C, and extension for 1 min 45 s at 68 °C; the final extension was 5 min at 68 °C. PCR products were cloned into the pGEM-T Easy Vector (Promega, Wisconsin, USA) sequenced and subcloned into

the pCDNA3 vector. P2X2-2bm was obtained together with other PCR products with changes in the sequence, using Recombinant Taq DNA Polymerase (Life Technologies, Texas, USA), conditions were as follows: initial denaturation for 5 min at 95 °C, then 40 amplification rounds of denaturation for 15 s at 95 °C, alignment for 20 s at 60 °C, and extension for 1 min 45 s at 72 °C; the final extension was 5 min at 72 °C. P2X2-2bm had two amino acid changes (codon 26 GAG>GGG; and codon185 CTG>CAG), one in the amino-terminal region (E26G) and another in the receptor's extracellular region (L185Q), such nucleotide changes were confirmed by several sequencing rounds using different primers. Early experiments showed us that these mutations increase the differences in ATP sensitivity and kinetics between this and P2X2-1a receptor. Therefore, we took advantage of this mutant in order to better distinguish these receptors here.

6.3. Preparation of *Xenopus laevis* oocytes

Frogs were anesthetized by immersions in a solution of 10 mM Tricaine (3-aminobenzoic acid ethyl ester; Sigma-Aldrich, MX) and oocytes were removed by dissection. Stages V-VI oocytes were manually defolliculated and placed in a storage saline solution, containing: Barth's solution (NaCl, 88 mM; Ca(NO₃)₂, 0.33 mM; KCl, 1 mM; CaCl₂, 0.41 mM; MgSO₄, 0.82 mM; NaHCO₃, 2.4 mM; and HEPES, 10 mM pH adjusted to 7.2-7.4 with NaOH). The cap and polyA P2X2 mRNA was synthesized with T7 mMessage mMachine (Life Technologies, Texas, USA). The mRNA was dissolved in RNase-free water at a final concentration of approximately 1 µg/µl, aliquoted and stored at -70°C until used. Cells were injected with 36 nl of cap and polyA P2X2 mRNA and incubated at 14°C for 12-36 h before

the electrophysiological experiments. The mRNA for P2X2-1a, P2X2-2bm or for both were injected in different groups of oocytes for every experiment. Injection of P2X2-1a/P2X2-2bm was performed in a ratio of 1:1.

6.4. Electrophysiological recordings

Membrane currents of oocytes were recorded using the two-electrode voltage clamp and the Axoclamp 2B amplifier (Molecular Devices). Recording electrodes consisted in glass pipettes (0.3-0.8 M Ω resistance) filled with 2 M KCl solution containing 10 mM EGTA. ATP-induced currents (IATP) were recorded at a holding potential of -60 mV and at room temperature (21-24°C).

6.5. Drugs Application

ATP was applied usually for 5-15 s or until reaching the maximal current. This nucleotide was washout between consecutive applications for at least 3 min. Pyridoxal 5-phosphate 6-azophenyl-2',4'-disulfonic acid (PPADS) was pre-applied 4 min to reach its steady effect (Guerrero-Alba *et al.*, 2010). Concentration-response curves were plotted using oocytes batches from at least three different frogs. During experiments, the recording chamber was continuously superfused with a standard external solution (NaCl, 88 mM; KCl, 2 mM; CaCl₂, 1 mM; MgCl₂, 1 mM; and HEPES, 5 mM pH adjusted to 7.2-7.4 with NaOH) at approximately 3 ml/min.

The external solution around the recorded cell was done by rapidly exchanging it using an eight-tube device. Each tube was connected to a syringe containing the control or an experimental solution. The tube with the control

solution was placed in front of the recorded cell and the external application of substances was applied by abruptly moving another tube in front of the cell, which was already draining the experimental solution. Tubes were moved using a Micromanipulator (WR-88; Narishigue Scientific Instrument Lab, Tokyo Japan). Substances were removed by returning to the control solution. External solution was delivered by gravity and the level of the syringes was regularly adjusted to decrease changes in flow rate.

6.6. Solutions and reagents

Salts and substances were all purchased from Sigma-Aldrich (Toluca, MX). ATP stock solutions (10 or 100 mM) were prepared in extracellular solution freshly every day. BzATP and PPADS stock solution (10 mM) was prepared using deionized water and stored frozen. The desired final drug concentration was obtained by diluting the stock solutions in extracellular solution before application. The pH was adjusted to 7.4 with NaOH when it was necessary.

6.7. Data analysis

Current normalization, in each cell, was done by considering as 100% responses to 1 mM (for P2X2-1a) or 3 mM (for P2X2-2bm) of ATP. Data are expressed as the mean \pm standard error of the mean (S.E.M.). Differences among multiple groups were examined using an ANOVA and a Bonferroni's post-hoc test. P values ≤ 0.05 were considered to be significant. Number of cells is represented by "n" and concentration-response curves were fitted, at least otherwise stated, with a three parametric logistic function (Kenakin, 1993).

Theoretical currents were calculated by mixing specific proportions of experimental currents through homomeric receptors (P2X2-1a:P2X2-2bm) recorded from two different oocytes, which were randomly paired. This was achieved by normalizing the adding currents after matching their maximal amplitude to 0.1, 0.5, and 0.9 if their desired final weight was 10, 50 or 90%, which correspond to ratios of 1:9, 1:1, and 9:1, respectively.

7. RESULTS

7.1. General properties of homomeric channels

ATP application evoked inward currents in oocytes expressing homomeric P2X2-1a and P2X2-2bm receptors in a concentration (0.001-10 mM) response manner (Fig. 4). Because maximal responses are virtually reached with 1 (-1350±254.6 nA, n=24) and 3 mM (-1898±255 nA, n=25) for P2X1-1a and P2X2-2bm, respectively, we normalized all currents considering maximal responses as 100%. When using data from individual cells expressing P2X2-1a receptor, a lower EC₅₀ (Table 2) was calculated than that of cells expressing P2X2-2bm receptors (Table 2).

Table 2. Summary of homomeric and coexpressed channel properties.

Receptor	Row Identifier	ATP EC ₅₀ (μM)	ATP Threshold (μM)	Hill Coefficient	Inhibition by 3 μM PPADS
P2X2-1a	*	14±3	0.41±0.06	2.35±0.48	82±5
P2X2-2bm	#	95±15*	0.69±0.1*	1.52±0.04*	37±7*
P2X2-1a like	&	21±3#	0.74 ± 0.14*	2.03±0.51#	21±4*
P2X2-2bm like		102±9&	0.77 ± 0.1*	1.64±0.12*,&	34±4*

Row identifier symbols are used to distinguish the data within a column that were significantly different ($P \leq 0.05$). No difference was found between other values. Mean EC₅₀s (μM) were calculated using individual cells. Means ± S.E.M., are shown. Number of cells varied from 11-21 for ATP EC₅₀ (in μM); 4-8 for ATP threshold concentration (in μM) and Hill Coefficients; and 4-7 for current-induced inhibition for PPADS (3 μM).

BzATP, an ATP analog, was also more potent on P2X2-1a than on P2X2-2bm receptors, with EC₅₀ values of 2.4±0.8 (n=5) and >100 μM (n=6), respectively (Fig 4C-D). The efficacy of BzATP appears to be smaller on P2X2-1a than on P2X2-2bm receptors.

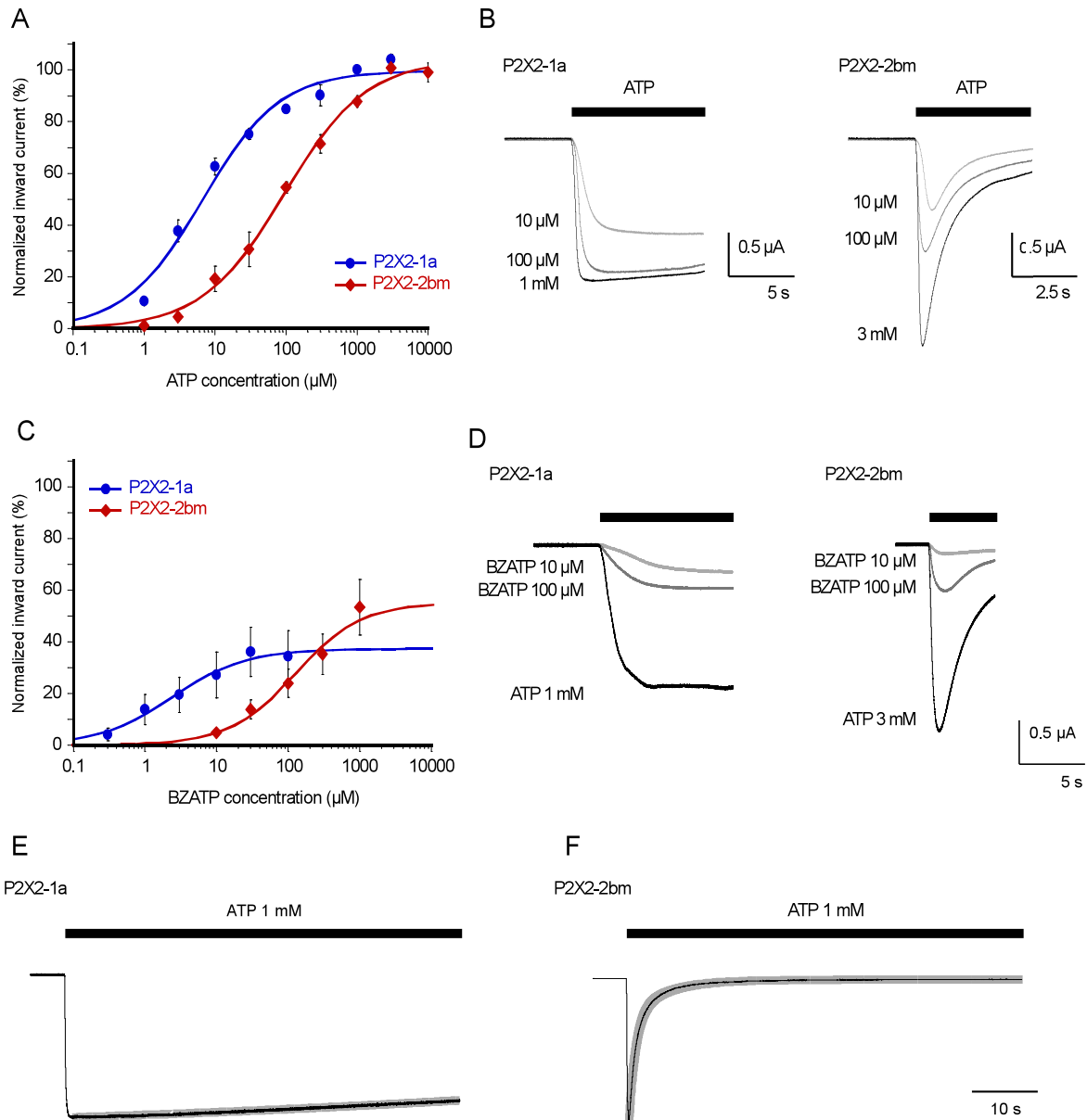


Figure 4. Homomeric channels have different kinetics and sensitivity to ATP and BzATP. **A)** Concentration-response curves for ATP currents mediated by P2X2-1a or P2X2-2bm receptors, data are well fitted to a three-parameters logistic model; each symbol represents the average value of at least six experiments. **B)** Representative traces of ATP induced-currents by P2X2-1a or P2X2-2bm. **C)** BzATP concentration-response curves for the same homomeric channels; each symbol represents the average value of at least four experiments. **D)** Representative traces of the BzATP induced-currents through either homomeric channels. **E)** Desensitization kinetics for P2X2-1a channels is well fitted to a single exponential function, currents induced by 1 mM ATP. **F)** Desensitization kinetics for

the P2X2-2bm is well fitted by the sum of two exponentials, in response to 1 mM ATP. Responses recorded from *Xenopus laevis* oocytes expressing P2X2-1a or P2X2-2bm, were normalized using as 100% the ATP current induced by 1 mM for P2X2-1a and 3 mM for P2X2-2bm. Vertical lines associated with symbols are S.E.M. of relative currents. Holding potential was -60 mV. Bars above traces indicate ATP application.

7.2. General properties of channels formed in coexpression experiments

When both P2X2-1a and P2X2-2bm were coexpressed in oocytes it became evident that at least two P2X channel populations were present in different oocytes, each with different ATP sensitivity, one similar to P2X2-1a (P2X2-1a like) and the other similar to P2X2-2bm (P2X2-2bm like). As it is shown in Figure 4A, 100 μ M ATP activates $85\pm 1.5\%$ of the maximal current observed for P2X2-1a receptors; whereas, at the same concentration activates only $55\pm 2.1\%$ of the maximal response of homomeric P2X2-2bm receptors (Fig. 4A-B). Therefore, at least three ATP concentrations (0.1, 1, and 3 mM) were used in co-expression experiments to check ATP sensitivity in every oocyte; Data were separated and ATP concentration-response curves were plotted (Fig. 5A-B). As it was calculated in individual cells, P2X2-1a like receptors have a higher sensitivity to ATP than P2X2-2bm like receptors.

BzATP activated both receptor populations with a concentration dependency similar to that of homomeric receptors (Fig 5C and D). Thus, BzATP has an EC_{50} value of 15 ± 1 (n=4) and >100 μ M (n=9) for P2X2-1a like and P2X2-2bm like receptors, respectively (Fig. 5C).

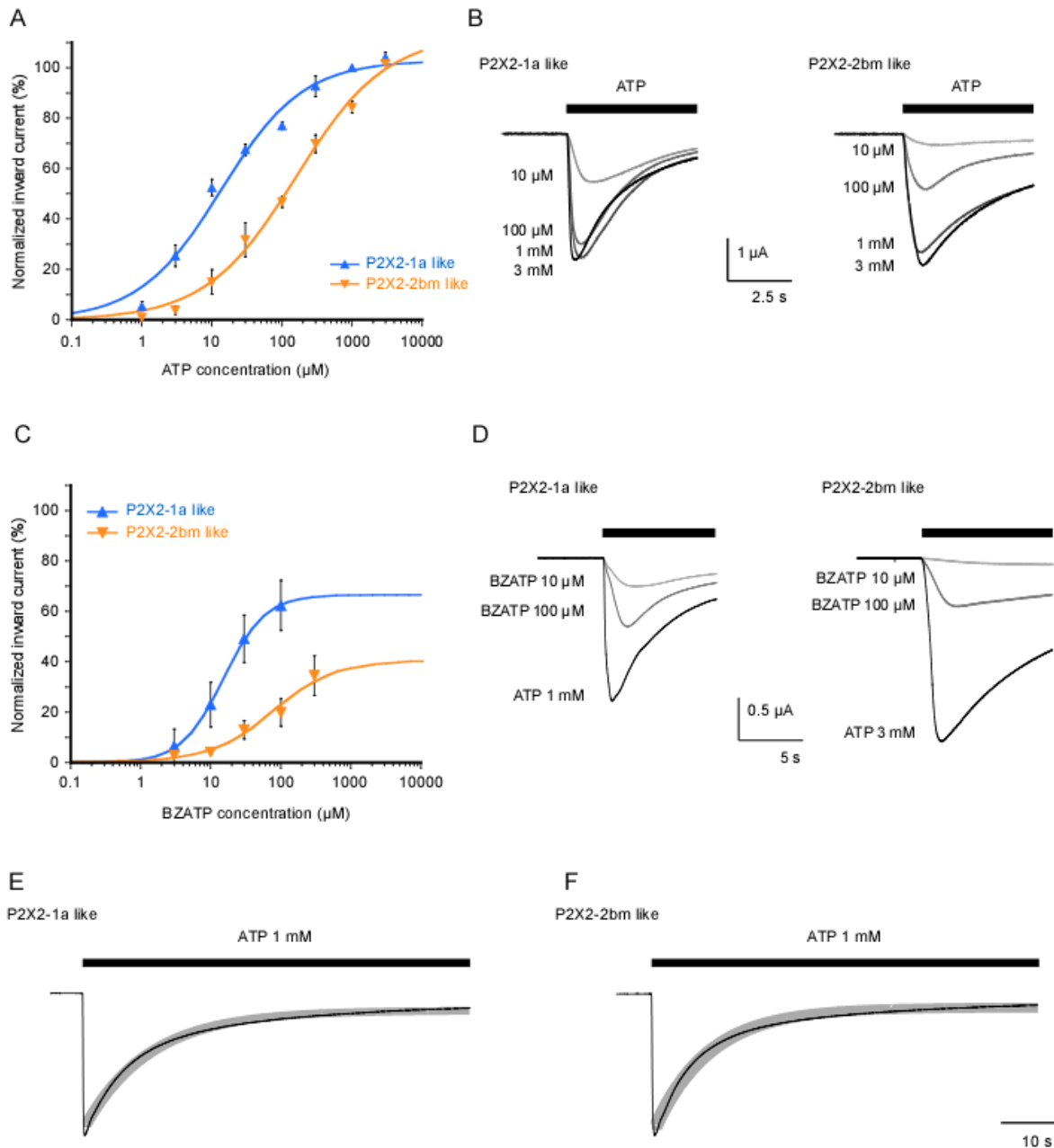


Figure 5. Channels formed by P2X2-1a/P2X2-2bm coexpression can be classified into at least two different groups. **A)** According to ATP sensitivity ("high or low"), responses from different oocytes were grouped. **B)** Representative traces of ATP induced-currents (0.01, 0.1, 1 and 3 mM) from oocytes coexpressing P2X2-1 and P2X2-2M subunits. **C)** BzATP concentration-response curves for heteromeric channels with high or low sensitivity to ATP. **D)** Representative traces of BzATP (10 and 100 μM) or ATP (1 or 3 mM) induced-currents from oocytes expressing type 1 and type 2 heteromeric channels. **E)** Desensitization kinetics for the heteromeric channel with higher sensitivity to ATP are

well fitted to a single exponential function. **F)** Desensitization kinetics for currents with lower sensitivity to ATP (1 mM ATP) are also well fitted by a single exponential function. Injection of P2X2-1/P2X2-2 was performed in a ratio of 1:1. For the concentration-response curves, data were normalized using as 100% those currents induced by 1 mM and 3 mM ATP, for the high and low sensitive currents. Each symbol represents the average value of at least four experiments, vertical lines associated with symbols are S.E.M. Holding potential was -60 mV and bars above traces indicate ATP application.

7.3. Current kinetics

Currents mediated by P2X2-1a channels showed virtually no desensitization during the continuous presence of ATP (Fig. 4E). Nevertheless, in some cells, a slow desensitization phase was observed, which was well fitted by an exponential function with a slower time constant (see Table 3 and Fig. 4E; n=6). P2X2-2bm receptor desensitization was well fitted by the sum of two exponentials functions (Table 3 and Fig. 4F, n=6).

Table 3. Desensitization kinetics parameters can predict when a homomeric channel contributes 10% to the maximal current

Currents	Ratio of P2X2-1a/ P2X2-2bm currents	Row Identifier	Desensitization kinetics		Decay kinetics
			t_1	t_2	t_1
Experimental	1 : 0	*	190±77		Complex behaviour
	0 : 1	#	2±0.4*	13.3±3.2	0.8±0.1
	P2X2-1a like	&	11±1.1*,#		2.6±0.2#
	P2X2-2bm like	∂	8.5±1.1*,#		1.8±0.4#
Theoretical	1 : 1	α	2.1±0.4*,&,∂	115±50#	
	9 : 1	β	1.8±0.9*,&,∂	49±15#,α	
	1 : 9		1.8±0.3*,&,∂	15±2.3α,β	

Row identifier symbols are used to distinguish the data within a column that were significantly different ($P \leq 0.05$). To obtain data for theoretical currents, experimental currents were normalized as it is described in Methods. Number of cells varied from 5 to 13 and t_{aus} were calculated by the best fitting of the currents to one or the sum of two exponential functions.

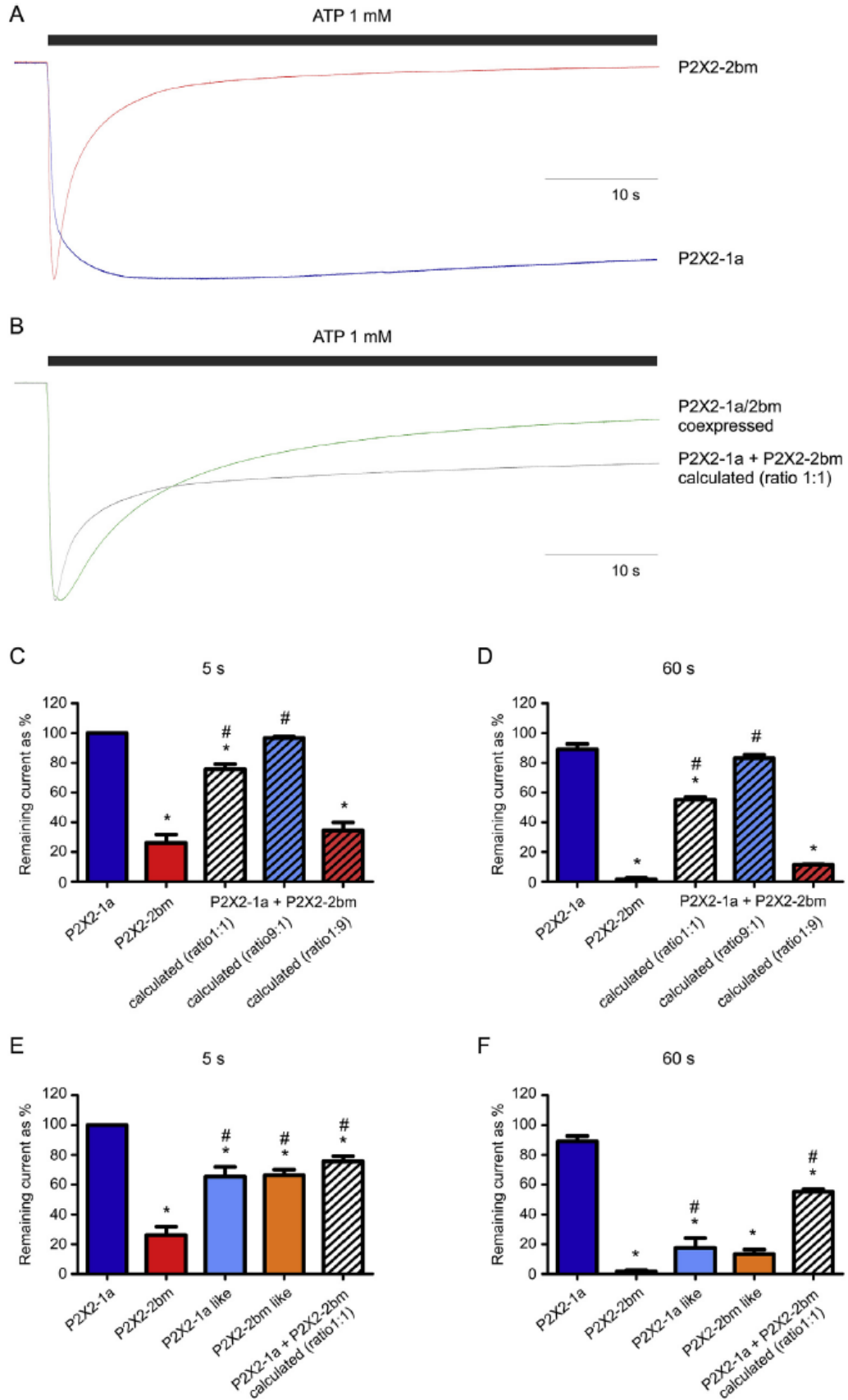


Figure 6. Current kinetics indicates that P2X2-1a like or P2X2-2bm like currents are not mediated by a significant expression of homomeric channels. A) Comparison of the kinetics for the mean currents from oocytes expressing either P2X2-1a (n=6) and P2X2-2bm (n=6) homomeric channels. **B)** Comparison of the kinetics for the mean currents from 13 oocytes expressing either P2X2-1a like or P2X2-2bm like channels and the expected kinetics if homomeric currents are added at a ratio of 1:1 (n=6). **C-F,** histograms showing the mean of percent of current (and S.E.M.) remaining after 5 and 60 s after starting the ATP application for homomeric channels, for both channel populations observed during coexpression experiments, and for theoretical currents obtained by adding P2X2-1a or P2X2-2bm at different ratios. Symbols above bars (*, and #), indicate P values equal or lower than 0.05, when data were compared with average data of P2X2-1a and P2X2-2bm, respectively.

Desensitization phase of ATP-induced currents mediated by P2X2-1a like receptors (n=13) and P2X2-2bm like receptors (n=13) was well fitted by a single exponential function and had virtually the same kinetics (Table 3, Fig. 5E-F). These currents desensitized with a significantly different kinetics than that of currents through individual homomeric channels (Fig. 6A-B, Table 3) or than kinetics of predicted currents when a similar proportion (ratio 1:1) of currents through homomeric channels were added (Fig. 6B, Table 3).

We also mixed currents through homomeric channels at ratios where one was predominant to see how this affected the kinetics. Calculated currents using a ratio of 9:1 of P2X2-1a and P2X2-2bm currents, respectively, were well fitted by the sum of two exponentials (Table 3) in 5 out of 12 experiments. In other five experiments, we observed currents with double peaks or with prominent humps and not fitting was performed on them. Only in 2 out of 12 experiments, currents were fitted with a single exponential function, displaying similar kinetics than

homomeric P2X2-1a receptor. This suggests that the desensitization kinetics can predict when P2X2-1a current represents only 10% of the total. Using a ratio of 1:9 of P2X2-1a and P2X2-2bm currents, respectively, we found that calculated currents were well fitted by the sum of two exponentials and have the same kinetics as P2X2-2bm receptor.

We also quantified and compared the currents remaining after 5 and 60 s of ATP application for homomeric receptors and for currents recorded during co-expression experiments. As it was expected, desensitization kinetics of homomeric channels are well correlated with the proportion of current remaining after 5 and 60 s. Thus, most of P2X2-1a current and a minimal proportion of P2X2-2bm were present after 5 and 60 s (Fig. 6C-D).

When currents of homomeric receptors were mixed at ratios (1:9 or 9:1) where one of them was dominant, remaining currents were very similar to the dominant current but when the mixing ratio was 1:1, these currents were significantly different than for homomeric channels (Fig. 6C-D). However, this mixing ratio, remaining currents were not different than currents from coexpression experiments at 5 s (Fig. 6E) but were significantly higher at 60 s (Fig. 6F). Opposite to this, remaining currents mediated by P2X2-1a like and P2X2-2bm like receptors had similar amplitudes and were significantly different than those observed at 5 s for both homomeric channels. At 60 s, however, they were significantly lower than currents through P2X2-1a receptor (Fig. 6E- F).

Currents mediated by P2X2-1a channels showed a rather complex decay after the removal of ATP (Table 3), which was fitted well to one exponential function in 8 out of 15 cells, however, the tau values showed a relatively wide

dispersion ($\tau_1=0.5$ up to 55 s). In 3 out of 15 cells, the decay was better fitted to the sum of two exponentials and in the other 4 cells it was not fitted even to the sum of three exponential functions. Currents mediated by the other three receptors (Table 3) were well fitted by a single exponential function. The kinetics decay of P2X2-1a like, and P2X2-2bm like receptors are significantly slower than that of P2X2bm receptor (Table 3).

7.4. ATP threshold and Hill coefficients

Fig. 7A shows the current amplitudes (as a percentage of maximal ATP response) induced by low ATP concentrations and Table 1 shows that the ATP threshold concentration (value calculated as the x axis intercept for individual cells, using a straight-line model, Fig. 7A) was significantly lower for P2X2-1a than for P2X2-2bm, P2X2-1a like or P2X2-2bm like receptors. No difference was observed between the last three receptors. Such observations are further evidence that oocytes with either P2X2-2bm like or P2X2-1a like currents do not express a measurable population of P2X2-1a homomeric receptors; otherwise, the ATP threshold concentration to activate such currents would have been similar to that of P2X2-1a receptors.

We plotted the log of such currents as a function of the log of these low ATP concentration and data were fitted with a straight-line function (Fig. 7B), as previously reported (Jiang *et al.*, 2003). The slopes of these fittings (Hill coefficients) are shown on Table 2. Consistent with idea that co-expression experiments generated two heteromeric receptor, one similar to P2X2-1a and another to similar to P2X2-2bm, Hill coefficients for P2X2-1a and P2X2-1a like

receptors were not different, similarly than for P2X2-2bm and P2X2-2bm like receptors (Table 2). However, these coefficients were significantly higher for P2X2-1a and P2X2-1a like receptors than those measured for P2X2-2bm and P2X2-2bm like receptors.

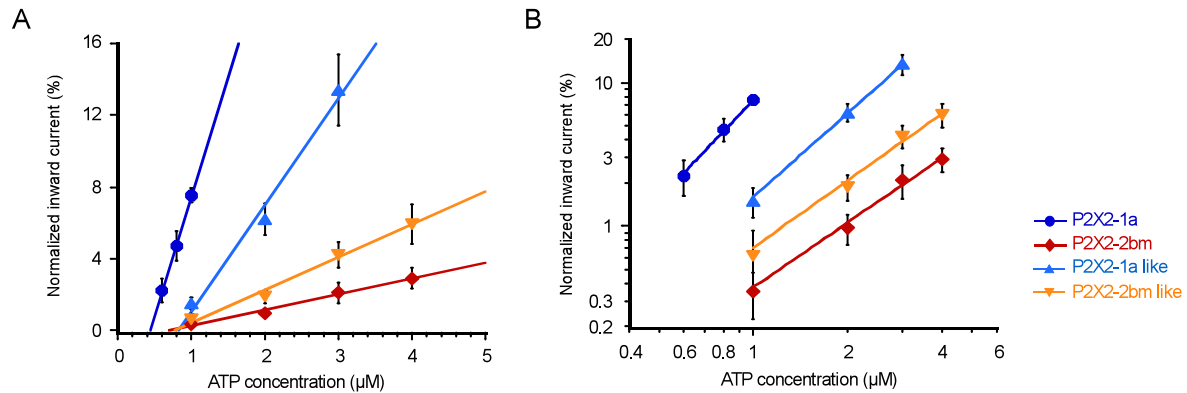


Figure 7. ATP threshold concentration for these currents suggests that a P2X2-1a homomeric channels does not significantly contribute to P2X2-1a like currents but their Hill coefficient suggest that P2X2-1a and P2X2bm subunits are required to activate P2X2-1a like P2X2-2bm like currents. A) The P2X2-1a homomeric receptor have the lowest ATP threshold concentration (0.41 μM) whereas, for the homomeric P2X2-2bm, the P2X2-1a like and P2X2-2bm like channels was virtually the same (0.69, 0.74 and 0.77 μM , respectively; see Table 1). Such a threshold was the calculated x axis intercept for individual cells, calculated by fitting the data to a straight-line model. **B)** Hill coefficients were not different between P2X2-1a and P2X2-1a like channels or between P2X2-2bm and P2X2-2bm like channels (see Table 1). However, this coefficient was significantly higher for P2X2-1a or P2X2-1a like channels than that of P2X2-2bm or P2X2-2bm like channels. Responses were fitted with a straight-line model. Currents were recorded at -60 mV in response to low concentrations of ATP as indicated and were normalized considering as 100% responses to 1 or 3 mM ATP, for high and low ATP sensitive currents, respectively. Symbols represent mean values of 4-8 experiments and the associated lines are S.E.M.

7.5. PPADS inhibitory effects

PPADS was seven folds more potent to inhibit P2X2-1a ($IC_{50}=0.7\pm 0.1 \mu\text{M}$) than P2X2-2bm ($IC_{50}=5\pm 0.3 \mu\text{M}$) homomeric receptors (Fig. 8A). The largest inhibitory differences are seen with 1 and 3 μM of PPADS, for instance, the latter concentration inhibited $82\pm 5\%$ ($n=4$) of the ATP-induced current mediated by P2X2-1a channels, while it only inhibited $37\pm 7\%$ ($n=4$) of the P2X2-2bm current. Using a concentration of 3 μM , we compared the PPADS inhibitory effect among homomeric and heteromeric receptors (Fig. 8B and Table 2). PPADS inhibitory effects on P2X2-1a like ($21\pm 4\%$, $n=4$) and P2X2-2bm like ($34\pm 4\%$, $n=7$) channels were not different than that observed for P2X2-2bm channels but this effect at these three channels was significantly lower than inhibition at P2X2-1a receptors. These findings rule out that the lower ATP sensitivity of P2X2-1a like receptors is due to a significant expression of homomeric P2X2-1a channels because these are highly sensitive to PPADS. Such findings make also unlikely that P2X2-1a channels mediate P2X2-2bm like currents.

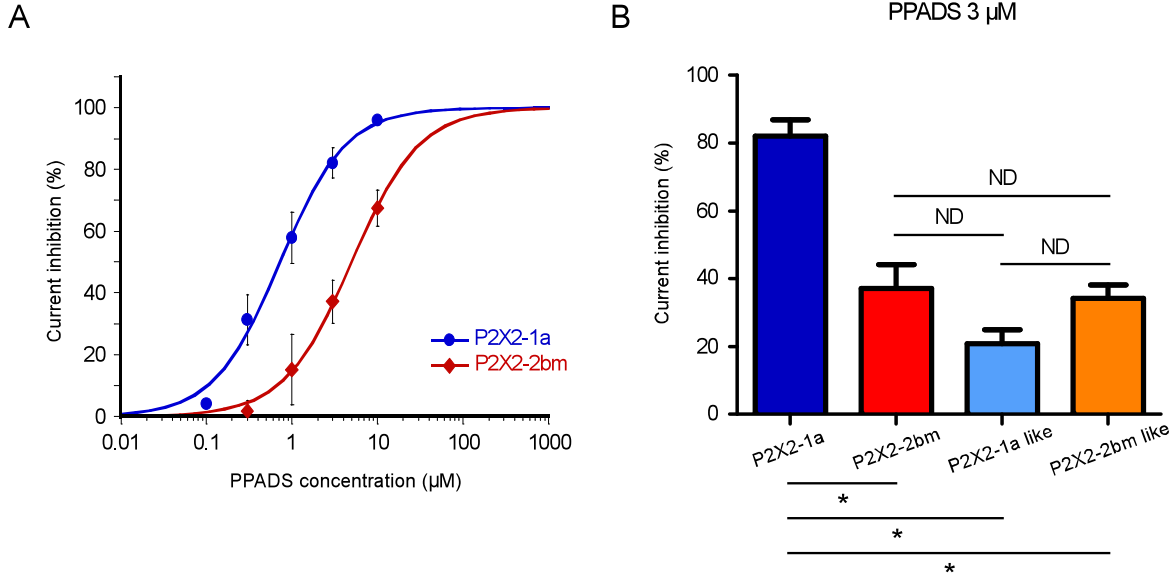


Figure 8. PPADS sensitivity of heteromeric channels is the same and similar to low sensitivity homomeric (P2X2-2bm) receptors. A) Concentration-response curves for the inhibitory effect of PPADS on ATP-induced currents (I_{ATP}). **B)** Inhibition of homomeric and heteromeric channels by 3 μM of PPADS. Currents were recorded at -60 mV in response to low concentrations of ATP as indicated and were normalized considering as 100% responses to 1 or 3 mM ATP, for high and low ATP sensitive currents, respectively. Symbols represent mean values of at least 4 experiments and the associated lines are S.E.M.

8. DISCUSSION

Our data indicates the formation of functional heteromeric channels with different stoichiometries when two splice variants of the P2X2 receptor were coexpressed in *Xenopus laevis* oocytes. Both heteromeric stoichiometries show the same desensitization kinetics indicating that it is enough to change a single subunit to modify this property. Previous experimental data indicated that ATP binding pocket is formed between two subunits, our observations indicates that a point mutation in one subunit can by itself be an important modulator for the binding pocket sensitivity, in agreement with previous reports (Hausmann *et al.*, 2012; Jiang *et al.*, 2003; Wilkinson *et al.*, 2006). Our data are compatible with a current model, which considers that activation of two binding sites by ATP is required to open P2X channels. However, binding to all three subunits might be required to inhibit P2X2 receptors by PPADS.

ATP concentration-response curves for P2X2-1a and P2X2-2bm like currents were monophasic suggesting that each of these currents is mediated by a single type of receptor. Various observations indicate that the higher ATP sensitivity of P2X2-1a like currents is not due to a significant expression of homomeric P2X2-1a channels during co-expression experiments, thus for P2X2-1a like current: i) the ATP threshold concentration was higher than for P2X2-1a current; ii) PPADS is less potent than at homomeric P2X2-1a channels; iii) the desensitization kinetics occurs more rapidly than for P2X2-1a current; iv) the remaining current amplitude, 5 and 60 s after ATP application, was lower than for

P2X2-1a current, similar findings were seen for predicted currents at ratios of 1:1 and 1:9 of P2X2-1a:P2X2-2bm currents, respectively, but opposite findings were noticed for ratio 9:1 currents; and v) the decay of P2X2-1a like current, after ATP removal, was well fitted by a single exponential function but occurs in a more complex manner in 66% of the recordings of P2X2-1a currents.

Similarly, several findings indicate that the lower ATP sensitivity of P2X2-2bm like current is not due to a significant expression of homomeric P2X2-2bm channels during co-expression experiments, thus for P2X2-2bm like current: i) desensitization kinetics is slower than for P2X2-2bm current; ii) its kinetics is virtually the same than that of P2X2-1a like receptors but their agonist sensitivity is significantly different; iii) the remaining current amplitude, 5 s after ATP application, was larger than for P2X2-2bm current and for predicted currents at a ratio of 1:9 of P2X2-1a:P2X2-2bm currents, respectively; iv) this remaining current, 60 s after ATP application, was lower than for predicted current at a ratio of 1:1 of these currents; and v) the decay of P2X2-2bm like currents, after ATP removal, was significantly lower than for P2X2-2bm currents. Therefore, a simpler explanation for our findings is that channels mediating P2X2-1a like and P2X2-2bm like currents are heteromeric and their different ATP sensitivity and different Hill coefficients could result from two different heteromeric stoichiometries.

It is also unlikely that both heteromeric stoichiometries are present in the same oocyte because ATP and BzATP concentration-response curves reveal clearly two populations of heteromeric channels very similar to either P2X2-1a or P2X2-2bm homomeric channels. Furthermore, Hill coefficients of heteromeric receptors are not different than those of homomeric receptors that they resemble.

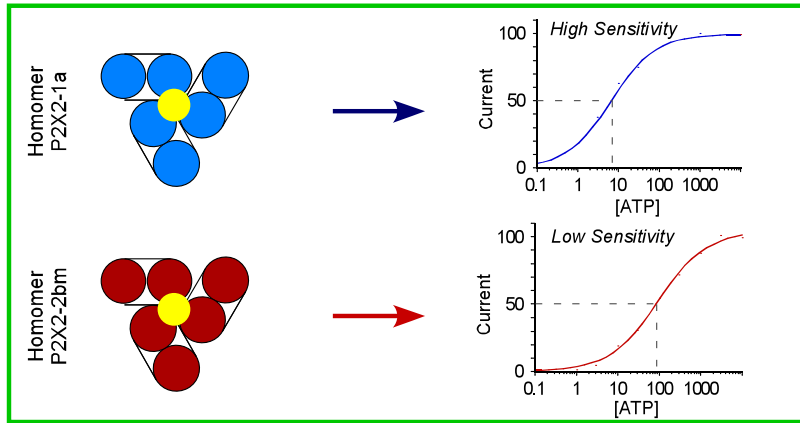
We do not know why a given oocyte prefers to express one stoichiometry versus the other one because we always microinjected a similar proportion of mRNA into the cells. Using atomic force microscopy, previous studies have shown the formation of heteromeric channels with different stoichiometries, in which the levels of subunits expression determines the prevalence of a specific stoichiometry (Barrera *et al.*, 2007). Furthermore, a recent article (Kowalski *et al.*, 2015) reports observations indicating that the availability of P2X2 and P2X3 subunits determined the stoichiometry of heterotrimeric P2X2/3 receptors. Therefore, it is possible that transduction of the mRNA injected in co-expression experiments occurs with different efficacy for both P2X2 isoforms in different cells, contributing to the fine-tuning of ATP signalling. However, further studies aim to investigate the precise mechanisms controlling the specificity of P2X receptors assemble are required. We proposed that the assembling of the two P2X2 splice variants reported might offer a good model for these type of studies if one considers that they share a similar structure.

Previous studies have characterized a single functional stoichiometry for heteromeric channels, such as P2X2/3 and P2X2/6 heteromers by using selective agonists to one subunit or mutagenesis that remove agonist sensitivity of one subunit (Hausmann *et al.*, 2012; Jiang *et al.*, 2003; Wilkinson *et al.*, 2006). Here we show that splice variants of the P2X2 receptor can form two different heteromeric stoichiometries. Thus, currents from co-expression experiments of P2X2-1a and P2X2-2bm subunits desensitized with a quite different kinetics than that of homomeric channels or than the kinetics expected if currents through homomeric channels are added, indicating that heteromeric receptors are being formed.

Because functional P2X channels are constituted as trimers of P2X subunits (Kawate *et al.*, 2009; North, 2002; Torres *et al.*, 1999), only two heteromeric stoichiometries are possible, the first by two P2X2-1a and one P2X2-2bm subunits (stoichiometry P2X2-1a/-2bm [2:1]) and the second by one P2X2-1a and two P2X2-2bm subunits (stoichiometry P2X2-1a/-2bm [1:2]). In agreement with the presence of these stoichiometries, we found heteromeric receptors with two different sensitivities to ATP, as well as different Hill coefficients, similar to that of the homomeric receptor that they resemble.

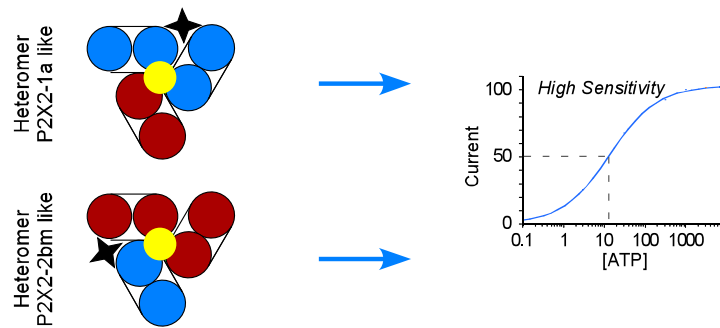
Three possible models of how trimeric P2X channels could be activated are indicated in Fig. 9B-D, these are: i) if channels open by activation of a single subunit, it would be expected that both receptor stoichiometries would be as sensitive as P2X2-1a (Fig. 9B) because this subunit is present in both possible heteromeric channels; ii) If channels open by activation of all three subunits, it would predict that both receptor stoichiometries would be as sensitive as P2X2-2bm (Fig. 9D) because this subunit is also present in both possible heteromeric channels; iii) Finally, if channels open by activation of two subunits both receptor stoichiometries would have different sensitivities, similar to those of the homomeric channels, as it was found here (Fig. 9C). Such an interpretation is on line with previous reports indicating that P2X2 receptors open when two, out of three, binding sites are activated (Hausmann *et al.*, 2012; Jiang *et al.*, 2003; Wilkinson *et al.*, 2006). Here we show that the ATP threshold concentration of both heteromeric channels is larger than that of P2X2-1a homomeric channels, compatible with the idea that binding to a single subunit (the most sensitive is P2X2-1a) is not enough

A Experimental data



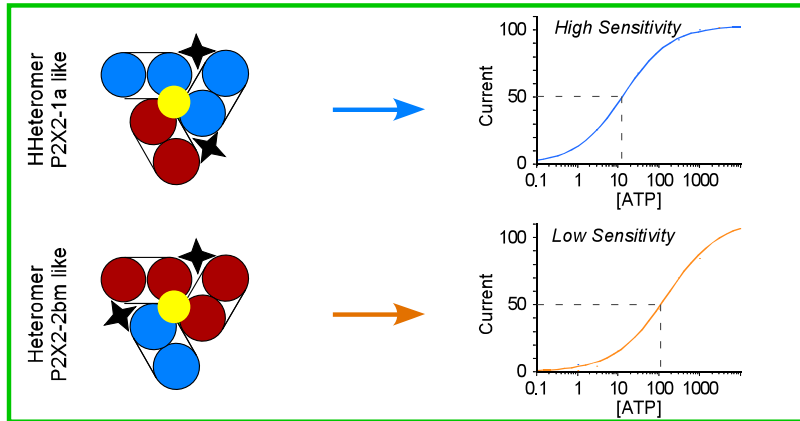
Both channels are activated in the same way with different sensitivity

B OPEN by Activation of a Single Subunit



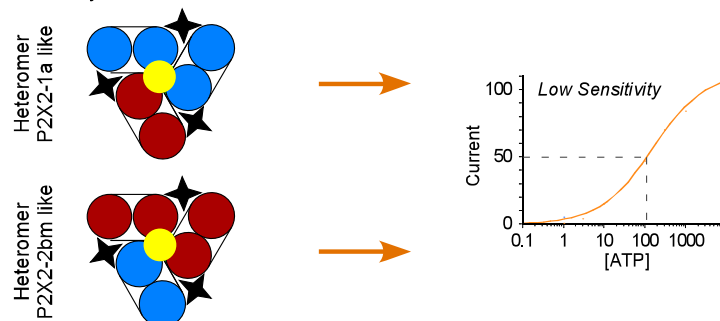
Expected if the channel was opened by the activation of **one** subunit

C OPEN by Activation of Two Subunits (Experimental data)



Expected if the channel was opened by the activation of **two** subunits

D OPEN by Activation of Three Subunits



Expected if the channel was opened by the activation of **three** subunits

Figure 9. Activation of P2X2 channels by occupancy of two ATP binding sites. Our data is compatible with a current model, according to which the activation of two binding sites (of three possible) is enough to activate P2X2 channel opening. **A)** Experimental ATP concentration response curves measured in P2X2-1a and P2X2-2bm homomeric receptors. Expected ATP concentration response curve if either of the two possible heteromeric channel stoichiometries are activated by the binding of one ATP molecule (indicated by the start; **B**), two (**C**), or three ATP molecules (**D**).

to activate the channels. In agreement with this interpretation, Hill coefficients were larger than unity for heteromeric and homomeric P2X2 channels.

PPADS is known to inhibit P2X receptor function in a complex noncompetitive manner by inducing allosteric changes when binding to an extracellular receptor domain (Chessell *et al.*, 1998; Li *et al.*, 1998; Michel *et al.*, 2000). Here, the inhibitory effect of PPADS is not different on both heteromeric and homomeric P2X2-2bm receptors, but homomeric P2X2-1a channels are more sensitive to PPADS. Following the same reasoning as for ATP (see previous paragraph and Fig. 9), this would imply that if this inhibitor would require to bind to one subunit to inhibit P2X2 receptors, PPADS would have the same potency on both heteromeric receptors as for P2X2-1a homomeric channels. If it would require to bind to two subunits, then would have the same high potency for the P2X2-1a like heteromeric receptor as for the P2X2-1a homomeric receptor but low potency for the P2X2-2bm like heteromeric receptor. If this PPADS would require to bind to all three subunits to inhibit P2X2 receptors, then PPADS would have the same potency on both heteromeric receptors because these two receptors involve a minimal of one P2X2-2bm subunit. Therefore, our data is consistent with a model, according to which, the allosteric changes induced by PPADS on P2X2 channels

(Chessell *et al.*, 1998; Li *et al.*, 1998; Michel *et al.*, 2000) would require its binding to all three subunits in order to inhibit ATP actions.

Desensitization kinetics of both heteromeric receptors was not different, indicating that the addition of a single subunit is enough to change these kinetics. While the occupancy of two binding sites of the P2X channels is associated with the opening of these, the third site occupancy is associated with the expansion observed in the pore formation by P2X2 and P2X7(Khadra *et al.*, 2013; Yan *et al.*); it has also been linked to the mechanism of desensitization of the channels using Alexa-647-ATP (Bhargava *et al.*, 2013). Such interpretation is in agreement with our data because in both heteromeric receptors reported here the third binding site would be composed of a P2X2-2bm subunit and that might be the reason why desensitization kinetics is the same in both stoichiometries.

Several studies have proposed that the ATP-binding site is shared between two subunits, so the sensitivity of the binding site would be determined by both subunits (Kawate *et al.*, 2009; Li *et al.*, 2010; Marquez-Klaka *et al.*, 2007; Roberts *et al.*, 2012; Roberts *et al.*, 2004; Roberts *et al.*, 2007). Our data does not refute this hypothesis but suggest that changes in one of these subunits, is enough to modulate agonist sensitivity.

9. CONCLUSION

Altogether, our observations indicate that two heteromeric channels can be expressed from two splice variants of the P2X2 receptor. Further experimental analysis is required to investigate why a given cell chooses to express only one stoichiometry. It is enough to change a single subunit to modify the desensitization kinetics of P2X2 channels. Our observations support a current model, according to which, ATP activation of two subunits can open P2X2 channel. However, PPADS appears to bind the three channel subunits in order to inhibit ATP effects on P2X2 receptors.

10. REFERENCES

- Aschrafi, A, Sadtler, S, Niculescu, C, Rettinger, J, Schmalzing, G (2004) Trimeric architecture of homomeric P2X2 and heteromeric P2X1+2 receptor subtypes. *J Mol Biol* **342**(1): 333-343.
- Barnes, NM, Hales, TG, Lummis, SC, Peters, JA (2009) The 5-HT3 receptor--the relationship between structure and function. *Neuropharmacology* **56**(1): 273-284.
- Barrera, NP, Henderson, RM, Murrell-Lagnado, RD, Edwardson, JM (2007) The stoichiometry of P2X2/6 receptor heteromers depends on relative subunit expression levels. *Biophys J* **93**(2): 505-512.
- Bhargava, Y, Nicke, A, Rettinger, J (2013) Validation of Alexa-647-ATP as a powerful tool to study P2X receptor ligand binding and desensitization. *Biochem Biophys Res Commun* **438**(2): 295-300.
- Boue-Grabot, E, Barajas-Lopez, C, Chakfe, Y, Blais, D, Belanger, D, Emerit, MB, Seguela, P (2003) Intracellular cross talk and physical interaction between two classes of neurotransmitter-gated channels. *J Neurosci* **23**(4): 1246-1253.
- Boyd, ST (2006) The endocannabinoid system. *Pharmacotherapy* **26**(12 Pt 2): 218S-221S.
- Brady, CA, Stanford, IM, Ali, I, Lin, L, Williams, JM, Dubin, AE, Hope, AG, Barnes, NM (2001) Pharmacological comparison of human homomeric 5-HT3A receptors versus heteromeric 5-HT3A/3B receptors. *Neuropharmacology* **41**(2): 282-284.
- Burnstock, G (1976a) Do some nerve cells release more than one transmitter? *Neuroscience* **1**(4): 239-248.
- Burnstock, G (2009) Purinergic cotransmission. *F1000 Biol Rep* **1**: 46.
- Burnstock, G (1976b) Purinergic receptors. *J Theor Biol* **62**(2): 491-503.
- Burnstock, G (2006) Purinergic signalling--an overview. *Novartis Found Symp* **276**: 26-48; discussion 48-57, 275-281.
- Connolly, CN, Wafford, KA (2004) The Cys-loop superfamily of ligand-gated ion channels: the impact of receptor structure on function. *Biochem Soc Trans* **32**(Pt3): 529-534.

Conroy, WG, Berg, DK (1995) Neurons can maintain multiple classes of nicotinic acetylcholine receptors distinguished by different subunit compositions. *J Biol Chem* **270**(9): 4424-4431.

Craig, AM, Banker, G (1994) Neuronal polarity. *Annu Rev Neurosci* **17**: 267-310.

Chessell, IP, Michel, AD, Humphrey, PP (1998) Effects of antagonists at the human recombinant P2X7 receptor. *Br J Pharmacol* **124**(6): 1314-1320.

Dustin, ML (2012) Signaling at neuro/immune synapses. *J Clin Invest* **122**(4): 1149-1155.

Erb, L, Weisman, GA (2012) Coupling of P2Y receptors to G proteins and other signaling pathways. *Wiley Interdiscip Rev Membr Transp Signal* **1**(6): 789-803.

Foord, SM, Bonner, TI, Neubig, RR, Rosser, EM, Pin, JP, Davenport, AP, Spedding, M, Harmar, AJ (2005) International Union of Pharmacology. XLVI. G protein-coupled receptor list. *Pharmacol Rev* **57**(2): 279-288.

Galligan, JJ (2002a) Ligand-gated ion channels in the enteric nervous system. *Neurogastroenterol Motil* **14**(6): 611-623.

Galligan, JJ (2002b) Pharmacology of synaptic transmission in the enteric nervous system. *Curr Opin Pharmacol* **2**(6): 623-629.

Goyal, RK, Chaudhury, A (2013) Structure activity relationship of synaptic and junctional neurotransmission. *Auton Neurosci* **176**(1-2): 11-31.

Greengard, P (2001) The neurobiology of slow synaptic transmission. *Science* **294**(5544): 1024-1030.

Guerrero-Alba, R, Valdez-Morales, E, Juarez, EH, Miranda-Morales, M, Ramirez-Martinez, JF, Espinosa-Luna, R, Barajas-Lopez, C (2010) Two suramin binding sites are present in guinea pig but only one in murine native P2X myenteric receptors. *Eur J Pharmacol* **626**(2-3): 179-185.

Guimaraes, MZ (2008) Isoform specificity of P2X2 purinergic receptor C-terminus binding to tubulin. *Neurochem Int* **52**(1-2): 314-320.

Hattori, M, Gouaux, E (2012) Molecular mechanism of ATP binding and ion channel activation in P2X receptors. *Nature* **485**(7397): 207-212.

Hausmann, R, Bodnar, M, Woltersdorf, R, Wang, H, Fuchs, M, Messemer, N, Qin, Y, Gunther, J, Riedel, T, Grohmann, M, Nieber, K, Schmalzing, G, Rubini, P, Illes, P (2012)

ATP binding site mutagenesis reveals different subunit stoichiometry of functional P2X2/3 and P2X2/6 receptors. *J Biol Chem* **287**(17): 13930-13943.

Jaffrey, SR, Snyder, SH (1995) Nitric oxide: a neural messenger. *Annu Rev Cell Dev Biol* **11**: 417-440.

Jarvis, MF, Khakh, BS (2009) ATP-gated P2X cation-channels. *Neuropharmacology* **56**(1): 208-215.

Jiang, LH, Kim, M, Spelta, V, Bo, X, Surprenant, A, North, RA (2003) Subunit arrangement in P2X receptors. *J Neurosci* **23**(26): 8903-8910.

Junger, WG (2011) Immune cell regulation by autocrine purinergic signalling. *Nat Rev Immunol* **11**(3): 201-212.

Kandel, ER, Schwartz, JH, Jessell, TM (2000) *Principles of neural science*. 4th edn. McGraw-Hill: New York.

Kawate, T, Michel, JC, Birdsong, WT, Gouaux, E (2009) Crystal structure of the ATP-gated P2X(4) ion channel in the closed state. *Nature* **460**(7255): 592-598.

Kenakin, TP (1993) *Pharmacologic analysis of drug-receptor interaction*. 2nd edn. Raven: New York.

Khadra, A, Tomic, M, Yan, Z, Zemkova, H, Sherman, A, Stojilkovic, SS (2013) Dual gating mechanism and function of P2X7 receptor channels. *Biophys J* **104**(12): 2612-2621.

Khakh, BS, North, RA (2006) P2X receptors as cell-surface ATP sensors in health and disease. *Nature* **442**(7102): 527-532.

Kim, M, Jiang, LH, Wilson, HL, North, RA, Surprenant, A (2001) Proteomic and functional evidence for a P2X7 receptor signalling complex. *EMBO J* **20**(22): 6347-6358.

King, BF, Townsend-Nicholson, A, Wildman, SS, Thomas, T, Spyer, KM, Burnstock, G (2000) Coexpression of rat P2X2 and P2X6 subunits in *Xenopus* oocytes. *J Neurosci* **20**(13): 4871-4877.

Koshimizu, T, Koshimizu, M, Stojilkovic, SS (1999) Contributions of the C-terminal domain to the control of P2X receptor desensitization. *J Biol Chem* **274**(53): 37651-37657.

Koshimizu, TA, Tsujimoto, G (2006) Functional role of spliced cytoplasmic tails in P2X2-receptor-mediated cellular signaling. *J Pharmacol Sci* **101**(4): 261-266.

Kowalski, M, Hausmann, R, Schmid, J, Dopychai, A, Stephan, G, Tang, Y, Schmalzing, G, Illes, P, Rubini, P (2015) Flexible subunit stoichiometry of functional human P2X2/3 heteromeric receptors. *Neuropharmacology* **99**: 115-130.

Lagerstrom, MC, Schioto, HB (2008) Structural diversity of G protein-coupled receptors and significance for drug discovery. *Nat Rev Drug Discov* **7**(4): 339-357.

Landis, DM (1988) Membrane and cytoplasmic structure at synaptic junctions in the mammalian central nervous system. *J Electron Microscop Tech* **10**(2): 129-151.

Le, KT, Babinski, K, Seguela, P (1998) Central P2X4 and P2X6 channel subunits coassemble into a novel heteromeric ATP receptor. *J Neurosci* **18**(18): 7152-7159.

Lewis, C, Neidhart, S, Holy, C, North, RA, Buell, G, Surprenant, A (1995) Coexpression of P2X2 and P2X3 receptor subunits can account for ATP-gated currents in sensory neurons. *Nature* **377**(6548): 432-435.

Li, M, Kawate, T, Silberberg, SD, Swartz, KJ (2010) Pore-opening mechanism in trimeric P2X receptor channels. *Nat Commun* **1**: 44.

Li, P, Calejesan, AA, Zhuo, M (1998) ATP P2x receptors and sensory synaptic transmission between primary afferent fibers and spinal dorsal horn neurons in rats. *J Neurophysiol* **80**(6): 3356-3360.

Liñan-Rico, A, Jaramillo-Polanco, J, Espinosa-Luna, R, Jimenez-Bremont, JF, Linan-Rico, L, Montano, LM, Barajas-Lopez, C (2012) Retention of a new-defined intron changes pharmacology and kinetics of the full-length P2X2 receptor found in myenteric neurons of the guinea pig. *Neuropharmacology* **63**(3): 394-404.

Lodge, D (2009) The history of the pharmacology and cloning of ionotropic glutamate receptors and the development of idiosyncratic nomenclature. *Neuropharmacology* **56**(1): 6-21.

Lynch, JW (2009) Native glycine receptor subtypes and their physiological roles. *Neuropharmacology* **56**(1): 303-309.

Marquez-Klaka, B, Rettinger, J, Bhargava, Y, Eisele, T, Nicke, A (2007) Identification of an intersubunit cross-link between substituted cysteine residues located in the putative ATP binding site of the P2X1 receptor. *J Neurosci* **27**(6): 1456-1466.

Michel, AD, Kaur, R, Chessell, IP, Humphrey, PP (2000) Antagonist effects on human P2X(7) receptor-mediated cellular accumulation of YO-PRO-1. *Br J Pharmacol* **130**(3): 513-520.

Millar, NS, Gotti, C (2009) Diversity of vertebrate nicotinic acetylcholine receptors. *Neuropharmacology* **56**(1): 237-246.

Nicke, A, Kerschensteiner, D, Soto, F (2005) Biochemical and functional evidence for heteromeric assembly of P2X1 and P2X4 subunits. *J Neurochem* **92**(4): 925-933.

North, RA (2002) Molecular physiology of P2X receptors. *Physiol Rev* **82**(4): 1013-1067.

Olsen, RW, Sieghart, W (2009) GABA A receptors: subtypes provide diversity of function and pharmacology. *Neuropharmacology* **56**(1): 141-148.

Pereda, AE (2014) Electrical synapses and their functional interactions with chemical synapses. *Nat Rev Neurosci* **15**(4): 250-263.

Roberts, JA, Allsopp, RC, El Ajouz, S, Vial, C, Schmid, R, Young, MT, Evans, RJ (2012) Agonist binding evokes extensive conformational changes in the extracellular domain of the ATP-gated human P2X1 receptor ion channel. *Proc Natl Acad Sci U S A* **109**(12): 4663-4667.

Roberts, JA, Evans, RJ (2004) ATP binding at human P2X1 receptors. Contribution of aromatic and basic amino acids revealed using mutagenesis and partial agonists. *J Biol Chem* **279**(10): 9043-9055.

Roberts, JA, Evans, RJ (2007) Cysteine substitution mutants give structural insight and identify ATP binding and activation sites at P2X receptors. *J Neurosci* **27**(15): 4072-4082.

Saul, A, Hausmann, R, Kless, A, Nicke, A (2013) Heteromeric assembly of P2X subunits. *Front Cell Neurosci* **7**: 250.

Stelmashenko, O, Lalo, U, Yang, Y, Bragg, L, North, RA, Compan, V (2012) Activation of trimeric P2X2 receptors by fewer than three ATP molecules. *Mol Pharmacol* **82**(4): 760-766.

Südhof, TC (2004) The synaptic vesicle cycle. *Annu Rev Neurosci* **27**: 509-547.

Südhof, TC, Rizo, J (2011) Synaptic vesicle exocytosis. *Cold Spring Harb Perspect Biol* **3**(12).

Tahirovic, S, Bradke, F (2009) Neuronal polarity. *Cold Spring Harb Perspect Biol* **1**(3): a001644.

Torres, GE, Egan, TM, Voigt, MM (1999) Hetero-oligomeric assembly of P2X receptor subunits. Specificities exist with regard to possible partners. *J Biol Chem* **274**(10): 6653-6659.

Torres, GE, Haines, WR, Egan, TM, Voigt, MM (1998) Co-expression of P2X1 and P2X5 receptor subunits reveals a novel ATP-gated ion channel. *Mol Pharmacol* **54**(6): 989-993.

Webb, TE, Bateson, AN, Barnard, EA (1993) Isolation and characterization of a novel family of G protein-coupled receptors. *Biochem Soc Trans* **21**(2): 199S.

Weisman, GA, Woods, LT, Erb, L, Seye, CI (2012) P2Y receptors in the mammalian nervous system: pharmacology, ligands and therapeutic potential. *CNS Neurol Disord Drug Targets* **11**(6): 722-738.

Wilkinson, WJ, Jiang, LH, Surprenant, A, North, RA (2006) Role of ectodomain lysines in the subunits of the heteromeric P2X2/3 receptor. *Mol Pharmacol* **70**(4): 1159-1163.

Yan, Z, Khadra, A, Li, S, Tomic, M, Sherman, A, Stojilkovic, SS Experimental characterization and mathematical modeling of P2X7 receptor channel gating. *J Neurosci* **30**(42): 14213-14224.

APPENDIX A

Josue Jaramillo-Polanco, Andr meda Li n-Rico, Rosa Espinosa-Luna, Juan F. Jim nez Bremont, Luis M. Monta o, Marcela Miranda-Morales, Carlos Barajas-L pez. **Heteromeric channels with different phenotypes are generated when coexpressing two P2X2 receptor isoforms**. Biochemical and Biophysical Research Communications. 477: 54-61, 2016.
<http://dx.doi.org/10.1016/j.bbrc.2016.06.020>



Contents lists available at ScienceDirect

Biochemical and Biophysical Research Communications

journal homepage: www.elsevier.com/locate/ybbrc

Heteromeric channels with different phenotypes are generated when coexpressing two P2X2 receptor isoforms



Josue Jaramillo-Polanco^a, Andr meda Li n n-Rico^a, Rosa Espinosa-Luna^a,
Juan F. Jim nez-Bremont^a, Luis M. Monta o^b, Marcela Miranda-Morales^c,
Carlos Barajas-L pez^{a,*}

^a Divisi n de Biolog a Molecular, Instituto Potosino de Investigaci n Cient fica y Tecnol gica, San Luis Potos , San Luis Potos , Mexico

^b Departamento de Farmacolog a, Facultad de Medicina, Universidad Nacional Aut noma de M xico, M xico DF, Mexico

^c Universidad Aut noma de San Luis Potos , SLP, Mexico

ARTICLE INFO

Article history:
Received 23 May 2016
Accepted 4 June 2016
Available online 6 June 2016

Keywords:
P2X receptors
P2X2 splice variants
Heterologous expression
P2X receptor activation
PPADS binding

ABSTRACT

To investigate if channels with different stoichiometry are formed from P2X2 receptor isoforms during their heterologous co-expression. The two-electrode voltage-clamp technique was used to measure ATP induced currents in *Xenopus laevis* oocytes. We used a mutant (P2X2-2bm) because its ATP sensitivity is lower than P2X2-2b receptors, which highlights the differences with its splice variant P2X2-1a. Currents through homomeric channels had significantly different Hill coefficients. P2XR are trimeric proteins with three agonist binding sites; therefore, only two homomeric and two heteromeric stoichiometries are possible when both P2X2 isoforms are coexpressed, the heteromeric channels might be formed by: **i)** 2(P2X2-1a)+1(P2X2-2bm); or **ii)** 1(P2X2-1a)+2(P2X2-2bm). Because P2X2 channels open when two binding sites are occupied, these stoichiometries are expected to have different ATP sensitivities. Thus, co-expressing both P2X2 isoforms, two oocyte populations were distinguished based on their sensitivity to ATP and Hill coefficients. For the first population (P2X2-1a like), the ATP EC₅₀ and the Hill coefficient were not different than those of homomeric P2X2-1a channels similarly, for the second population (P2X2-2bm like), these variables were also not different than for those of homomeric P2X2-2bm channels. Various findings indicate that homomeric channel expression is not responsible for such differences. Our observations indicate that two heteromeric channels can be assembled from two P2X2 receptor isoforms. Our data support a current model, according to which, ATP activation of two subunits can open P2X2 channel. However, PPADS appears to bind to all three subunits in order to inhibit ATP effects on P2X2 receptors.

  2016 Published by Elsevier Inc.

APPENDIX B

Andrómeda Liñán-Rico, Josue Jaramillo-Polanco, Rosa Espinosa-Luna R, Juan F. Jiménez-Bremont, Liliana Liñán-Rico, Luis M. Montaña, Carlos Barajas-López. **Retention of a new-defined intron changes pharmacology and kinetics of the full-length P2X2 receptor found in myenteric neurons of the guinea pig.** *Neuropharmacology*. 63: 394-404, 2012.
<http://dx.doi.org/10.1016/j.neuropharm.2012.04.002>



Retention of a new-defined intron changes pharmacology and kinetics of the full-length P2X2 receptor found in myenteric neurons of the guinea pig

A. Liñan-Rico^a, J. Jaramillo-Polanco^a, R. Espinosa-Luna^a, J.F. Jiménez-Bremont^a, L. Liñan-Rico^a, L.M. Montaña^b, C. Barajas-López^{a,*}

^a División de Biología Molecular, Instituto Potosino de Investigación Científica y Tecnológica (IPICYT), Camino a la Presa San José 2055, Col. Lomas 4a Sección, CP78216 San Luis Potosí, SLP, Mexico

^b Departamento de Farmacología, Facultad de Medicina, Universidad Nacional Autónoma de México, México DF, Mexico

ARTICLE INFO

Article history:

Received 16 February 2012

Received in revised form

29 March 2012

Accepted 1 April 2012

Keywords:

ATP

P2X2 receptors

Alternative splicing

Intron retention

Myenteric neurons

Guinea pig

P2x2 gene

ABSTRACT

P2X2 plays an important role in ATP signaling in guinea pig myenteric plexus. Here, we cloned and characterized three P2X2 isoforms expressed in myenteric neurons. RT/PCR was used to amplify the cDNA of P2X2 variants. These were expressed in *Xenopus* oocytes, and nucleotide-induced membrane currents were recorded with the two-electrode voltage clamp technique. Three P2X2 cDNAs were identified in myenteric single neurons, named P2X2-1, P2X2-2 and P2X2-4. Based on the analysis of the structural organization of these variants we predicted that P2X2-2 is the fully processed variant, which lead us to propose a new exon-intron arrangement of P2X2 receptor gene with 12 exons and 11 introns. In agreement with this new model, the intron 11 is retained in P2X2-1 and P2X2-4 variants by alternative splicing. Expression of P2X2-1, P2X2-2 and P2X2-4 were found in 92, 42 and 37%, respectively, out of 40 analyzed single neurons. P2X2-4 does not form functional channels, and homomeric channels formed by P2X2-1 and P2X2-2 have different pharmacological profile. Thus, the former receptor is more sensitive to ATP, BzATP, and PPADS, whereas, suramin inhibited both receptors in a biphasic- and monophasic-manner, respectively. α,β -meATP has very low efficacy on either channel. Furthermore, ionic currents mediated by P2X2-1 have slower desensitization than P2X2-2. These results indicate that P2X2-1 was the most common P2X2 transcript in myenteric neurons and displays significant phenotypical changes implicating that retention of the intron 11 plays a major role in ATP signaling in the intestinal myenteric plexus.

© 2012 Elsevier Ltd. All rights reserved.

APPENDIX C

Raúl Loera-Valencia R, Josué Obed Jaramillo-Polanco, Andrómeda Liñán-Rico, María Guadalupe Nieto Pescador, Juan Francisco Jiménez Bremont, Carlos Barajas-López. **Genomic organization of purinergic P2X receptors.** *Pharmacology & Pharmacy*, 6, 341-362. 2015.
<http://dx.doi.org/10.4236/pp.2015.68036>

Genomic Organization of Purinergic P2X Receptors

Raúl Loera-Valencia, Josué Obed Jaramillo-Polanco, Andrómeda Linan-Rico, María Guadalupe Nieto Pescador, Juan Francisco Jiménez Bremont, Carlos Barajas-López*

División de Biología Molecular, Instituto Potosino de Investigación Científica y Tecnológica, San Luis Potosí, México
Email: cbarajas@ipicyt.edu.mx

Received 18 May 2015; accepted 11 August 2015; published 14 August 2015

Copyright © 2015 by authors and Scientific Research Publishing Inc.
This work is licensed under the Creative Commons Attribution International License (CC BY).
<http://creativecommons.org/licenses/by/4.0/>



Open Access

Abstract

Purinergic P2X receptors are a family of ligand-gated cationic channels activated by extracellular ATP. P2X subunit protein sequences are highly conserved between vertebrate species. However, they can generate a great diversity of coding splicing variants to fulfill several roles in mammalian physiology. Despite intensive research in P2X expression in both central and peripheral nervous system, there is little information about their homology, genomic structure and other key features that can help to develop selective drugs or regulatory strategies of pharmacological value which are lacking today. In order to obtain clues on mammalian P2X diversity, we have performed a bio-informatics analysis of the coding regions and introns of the seven P2X subunits present in human, simian, dog, mouse, rat and zebrafish. Here we report the arrangements of exon and intron sequences, considering its number, size, phase and placement; proposing some ideas about the gain and loss of exons and retention of introns. Taken together, these evidences show traits that can be used to gain insight into the evolutionary history of vertebrate P2X receptors and better understand the diversity of subunits coding the purinergic signaling in mammals.

Keywords

Alternative Splicing, Intron, Genomic Organization, P2X, Purinergic Signalling

1. Introduction

Purinergic P2X receptors are a family of ligand-gated cationic channels activated by extracellular ATP [1].

*Corresponding author.

How to cite this paper: Loera-Valencia, R., Jaramillo-Polanco, J.O., Linan-Rico, A., Pescador, M.G.N., Bremont, J.F.J. and Barajas-López, C. (2015) Genomic Organization of Purinergic P2X Receptors. *Pharmacology & Pharmacy*, 6, 341-362.
<http://dx.doi.org/10.4236/pp.2015.68036>

Seven subunits have been identified so far in mammalian species (P2X₁₋₇), and they are involved in numerous physiological roles like peristalsis, platelet aggregation, pain sensation, immune response and development [1]-[5]. To form a functional channel, P2X subunits assemble as homo or heteromeric trimers [6]. The pharmacological properties of the assembled P2X receptor vary in function to subunit composition [7] [8]. The subunit stoichiometry has a different arrangement among tissue in a given organism, and different composition among species, for example, the enteric nervous system of the rat, mouse and guinea pig expresses P2X₂/P2X₃ heteromeric receptors [6] [9] while sensory ganglia and heart of rodents and humans express homomeric P2X₃ receptors [10] [11]. In addition, P2X receptors can assemble from tissue specific splicing variants of its messenger RNA [1].

The physiological role of P2X receptors seems to be the same for different species of mammals: purinergic neurotransmission. Even when the population of P2X subunits in a tissue between two species may vary [12] [13], the P2X subunit protein sequences are highly conserved between vertebrate species [14]. Sequences correspond to cysteine allowing disulfide bonds, and transmembrane domains I and II and a YXXXX motif in the c-terminus of each protein are specially conserved among species [1].

Despite the high conservation of P2X subunits between vertebrates, the analysis of completely sequenced genomes of non-vertebrate model organisms like *Drosophila melanogaster*, *Caenorhabditis elegans* and *Apis mellifera* show no homologues to P2X receptors [14] [15]. Previous works have hypothesized that ATP is a very early neurotransmitter in evolution of vertebrates with a single P2X receptor as ancestor [16]. Phylogeny suggests that diversification of seven P2X subunits presented in mammals is an evolutionary event subsequent to the split between vertebrates and invertebrates [17]. There are evidences showing that non-vertebrates like *Schistosoma mansoni* have P2X homologues [18], so it's been proposed that arthropods and nematodes lose their P2X homologues later in their own evolution [17].

The increase of genomic data is available from unicellular, and simple-celled organisms have substantially improved our knowledge about the evolutionary path of purinergic transmission and P2X receptors [14], however, to date there exist no selective agonist or modulator for the P2X family with few exceptions currently under testing [19]. Because of this, we have performed a bioinformatics analysis of the coding regions and introns of the seven P2X genes being presented in human, simian, dog, mouse, rat and zebrafish. Here we report the arrangements of exon and intron sequences, considering its number, size, phase and placement; proposing some ideas about the gain and loss of exons and retention of introns. We expect that these evidences show traits, which can be used to gain insight into the primary structure of vertebrate P2X receptors and help design selective pharmacological drugs and single-subunit regulatory strategies.

2. Materials and Methods

2.1. Analysis of Genomic Sequences of P2X Receptors

Several genomic cDNA sequences encoding P2X receptors of *Homo sapiens*, *Pan troglodytes*, *Rattus norvegicus*, *Mus musculus*, *Canis lupus familiaris*, *Danio rerio* and *Anolis carolinensis* for P2X₆ (given the absence of *Danio rerio*'s P2X₆ receptor) were obtained from the NCBI (National Center for Biotechnology Information, Bethesda, MD, USA; <http://www.ncbi.nlm.nih.gov>) database and only a few of them from Ensembl database (www.ensembl.org). Each of the P2X receptors sequence and Gen Bank accession no. of each organism are shown in Supplementary Table S1.

All the P2X genes of the organisms mentioned above were analyzed for the determination of genomic organization, including the size, gain and loss of exons, as well as intron number, size, loss, retention, placement and phase. The exon-intron organization was obtained from the analysis of the information available in the NCBI database.

Pairwise alignments were conducted in order to establish exon and intron sequence identities among species using the Needleman-Wunsch (global) and Smith-Waterman (local) alignment programs at the EBI (European Bioinformatics Institute, Cambridge, UK; <http://www.ebi.ac.uk>) database. Microsynteny between P2X receptor genes from the different organisms was assembled using the information present in the NCBI database chromosome image (<http://www.ncbi.nlm.nih.gov/gene>). Prediction of possible transposable element sequences within the P2X genes was performed using Blastn algorithm of the NCBI database.

2.2. Molecular Phylogenetic Analysis

The aminoacid sequences of the P2X receptors were aligned and the respective phylogenetic tree constructed

Table 1. Gene information of P2X subunits used in the gene structure and phylogeny analyses.

P2X Gene	Gene length (bp)	Gene without UTR (bp)	mRNA (bp)	Messenger without UTR (bp)	Protein (aa)	mRNA Accession	Protein Accession	Status	Chromosome
P2X₁									
MUS	16,053	14,812	2441	1200	399	NM_008771.3	NP_032797.3	validated	11
RNO	15,053	13,782	2539	1200	399	NM_012997.2	NP_037129.1	provisional	10
HSA	20,076	18,412	2910	1200	399	NM_002558.2	NP_002549.1	reviewed	17
CAF	NE	13,559		1200	399	XM_548344.1	XP_548344.1	predicted	9
MMU	21,173	20,436	1937	1200	399	XM_001092205.2	XP_001092205.1	predicted	16
DAR	NE	27,735		1197	398	ENSDART00000011544	ENSDARP00000010823	provisional	5
P2X₂									
MUS	3224	2763	1712	1251	416	NM_001164833.1	NP_001158305.1	validated	5
RNO	3195	2782	1625	1212	403	Y10473	CAA71499.1	provisional	12
HSA	3570	3156	1629	1215	404	NM_174873.1	NP_777362.1	reviewed	12
CAF	NE	2757		1185	394	XM_851798.1	XP_856891.1	predicted	26
MMU	3485	3071	1626	1212	403	XM_001082602.2	XP_001082602.2	predicted	11
DAR	14,522	14,433	1292	1203	400	NM_198983.1	NP_945334.1	provisional	5
P2X₃									
MUS	39,283	36,287	4190	1194	397	NM_145526.2	NP_663501.2	validated	2
RNO	42,707	40,151	3773	1194	397	NM_031075.1	NP_112337.1	provisional	3
HSA	31,601	31,446	1349	1194	397	NM_002559.2	NP_002550.2	reviewed	11
CAF	NE	25,834		1194	397	XM_540614.1	XP_540614.1	predicted	18
PTR	33,271	32,483	1982	1194	397	XM_001136930.1	XP_001136930.1	predicted	11
DARa	15,454	14,977	1724	1233	410	NM_131623.1	NP_571698.1	provisional	14
DARb	12,235	10,544	2920	1239	412	NM_198986.2	NP_945337.2	provisional	1
P2X₄									
MUS	21,488	20,660	1995	1167	388	NM_011026.2	NP_035156.2	validated	5
RNO	17,652	16,846	1997	1167	388	NM_031594.1	NP_113782.1	provisional	12
HSA	24,246	23,385	2043	1167	388	NM_002560.2	NP_002551.2	reviewed	12
CAF	16,697	16,185	1679	1167	388	XM_543389.2	XP_543389.1	predicted	26
PTR	25,836	24,971	2032	1167	388	XM_509437.2	XP_509437.2	predicted	12
DARa	9193	9046	1330	1170	389	NM_153653.1	NP_705939.1	provisional	21
DARb	7918	7883	1243	1206	401	NM_198987.1	NP_945338.1	provisional	8
P2X₅									
MUS	12,158	11,238	2293	1368	455	NM_033321.3	NP_201578.2	validated	11
RNO	11,610	10,569	2436	1368	455	NM_080780.2	NP_542958.2	provisional	10
HSA	23,063	22,138	2206	1269	422	NM_002561.2	NP_002552.2	reviewed	17
CAF	13,312	12,894	1705	1287	428	XM_548343.2	XP_548343.2	predicted	9
PTR	26,312	20,930	2195	1269	422	XM_511272.2	XP_511272.2	predicted	17
DAR	23,322	22,426	2367	1443	481	NM_194413.1	NP_919394.1	provisional	5
P2X₆									
MUS	10,128	8952	2362	1170	389	NM_011028.2	NP_035158.2	validated	16
RNO	10,037	8919	2331	1170	389	NM_012721.2	NP_036853.2	validated	11
HSA	12,839	11,443	2754	1326	441	NM_005446.3	NP_005437.2	reviewed	22

Continued

CAF	NE	8980		1230	410	ENSECAFT00000023919	ENSCAFP00000022204	predicted	26	
MMU	NE	12,957		1317	438	XM_001084368.2	XP_001084368.1	predicted	10	
ACA	NE	4774		1167	389	ENSACAT00000011065	ENSACAP00000010841	predicted	NE	
P2X₇										
MUS		40,374	37,231	4931	1788	595	NM_011027.2	NP_035157.2	validated	5
RNO		43,128	41,366	3540	1788	595	NM_019256.1	NP_062129.1	provisional	12
HSA		53,724	51,832	3680	1788	595	NM_002562.5	NP_002553.3	reviewed	12
CAF	NE	42,756		1788	595	NM_001113456.1	NP_001106927.1	provisional	26	
MMU		55,453	54,038	3203	1788	595	XM_001092531.2	XP_001092531.1	predicted	11
DAR		20,914	20,847	1860	1791	596	NM_198984.1	NP_945335.1	provisional	8
P2X₈										
DAR		27,994	27,989	1178	1173	390	NM_198985.1	NP_945336.1	provisional	15

Table 2. Percent identity of mouse P2X paralogs (clustal W).

		1	2	3	4	5	6	7
1	musP2X ₁	x	32.3	37.5	47.4	36.1	39.3	31.8
2	musP2X ₂		x	41.3	39.4	40.1	35	28.1
3	musP2X ₃			x	40.5	38.3	35.2	30.5
4	musP2X ₄				x	45.9	41	40.5
5	musP2X ₅					x	44.7	27.3
6	musP2X ₆						x	29
7	musP2X ₇							x

using the software MEGA version 4.0 with the maximum parsimonia method (500 bootstrap).

3. Results and Discussion

The seven P2X subunits (1 - 7) in mammals are diverse in size and gene organization. P2X₂ is the smallest of the subunits, with a 2.78 Kb transcript. The longest is P2X₇ with 37.23 Kb (see **Table 1**). However, the ORF size of the seven subunits from the species analyzed in this work has an average of 1.3 Kb without untranslated sequences—P2X₄ has the smallest transcript with 1.16 Kb and P2X₇ possess the longest transcript of 1.78 Kb, their aminoacid sequences are 388 and 595 residues respectively. Mainly, the difference in size between P2X subunits is related to the size of their C-terminus domains.

3.1. Genomic Organization of P2X Genes of the Mouse

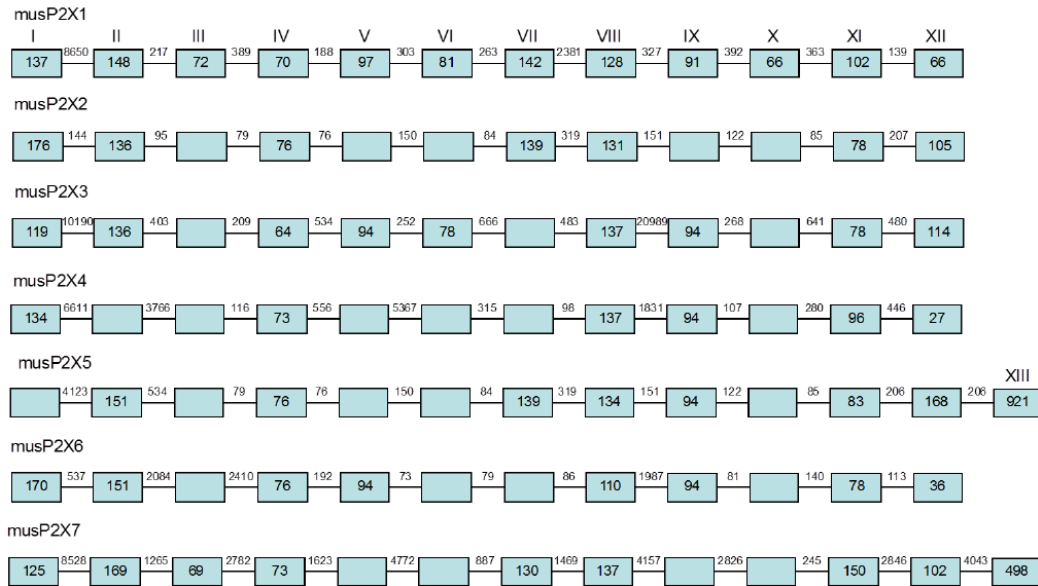
The P2X subunits of mouse consist of 12 to 13 exons and 11 to 12 introns according to the reported sequences of Gene Bank (**Figure 1(a)**). In detail, subunits P2X₁, P2X₂, P2X₃, P2X₄ and P2X₆ have 12 exons and 11 introns, whereas P2X₅ and P2X₇ have an arrangement of 13 exons and 12 introns.

Despite the differences of aminoacid sequences among P2X subunits (below 50% identity, **Table 2**), exon size trends to be conserved from Exons III to X, which is the middle portion of the ORF; with exons III and X as the most conserved (most of them are 72 and 66 nucleotides long respectively), whereas the last exons are the most variable in size (**Figure 1(a)**). In counterpart, the introns have a high variability in size and sequence, this could be the cause of identity differences at genomic DNA level between P2X genes in mice. The conservation of exon size and high variability of intron length has been previously described in other gene families in previous works [20], which are evidence of evolutionary mechanisms affecting their gene structure.

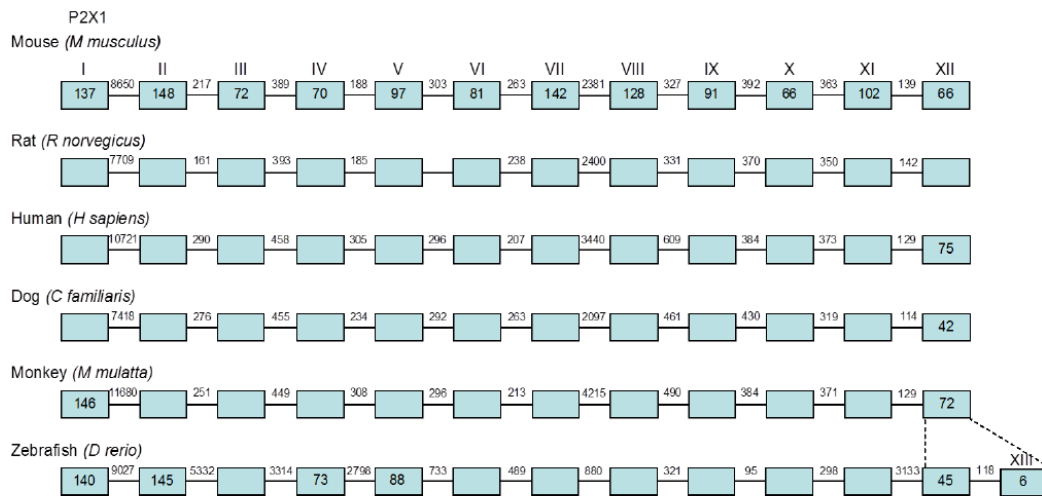
Exon III codes for 24 aminoacids located in the extracellular loop, and exon X forms the first half of the transmembrane region II, part of the channel pore [21]. In counterpart, the most variable regions of the exons of P2X subunits are those involved in traffic, receptor desensitization, cytoskeleton binding, receptor-receptor in-

teraction and regulatory proteins, which contribute to the diversity of function of the assembled P2X receptors.

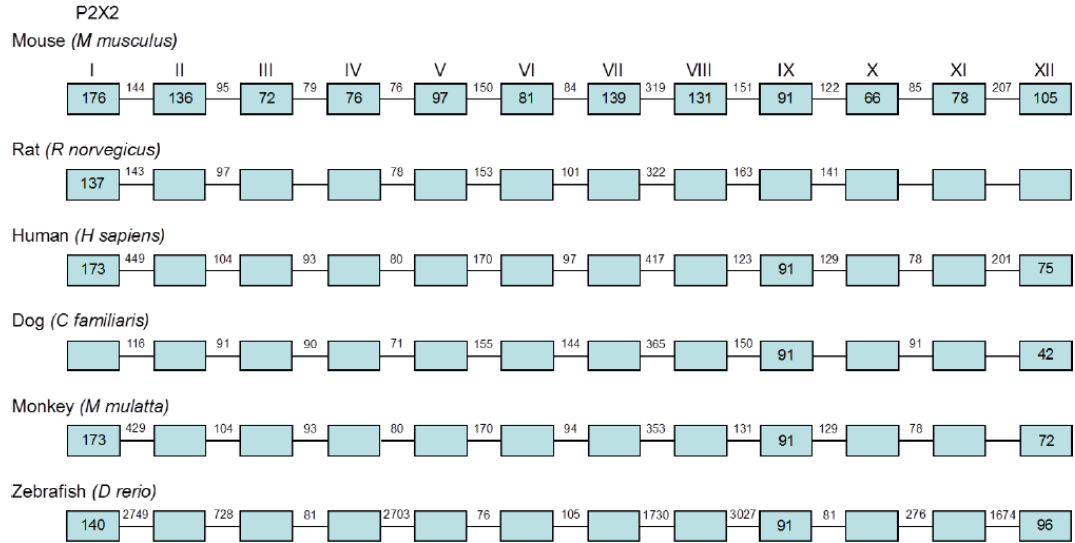
Intron size among P2X subunits in mouse is highly variable, with P2X₂ as the gene with the shortest introns (76 to 319 bp). Previous works showed shorter introns in constitutive genes compared to those of low expression [22] [23]. This is explained by the naturally selected gene compression since transcription and mRNA processing are slow and energetically costly processes [22] [24]. The small intron size of P2X₂ correlates with its high prevalence in cells responsive to purinergic signaling like neurons of the peripheral nervous system [25]. On the other hand, subunits like P2X₃ seem to be present mostly at early stages of development and scarcely found in adult neurons according to other works [5] [26]-[28] and to our single cell PCR results performed in myenteric neurons of mice [29]. These results correlate with the longer size of P2X₃ introns in a gene that is not as widely expressed by neural cell types and does not need high efficiency transcription rates.



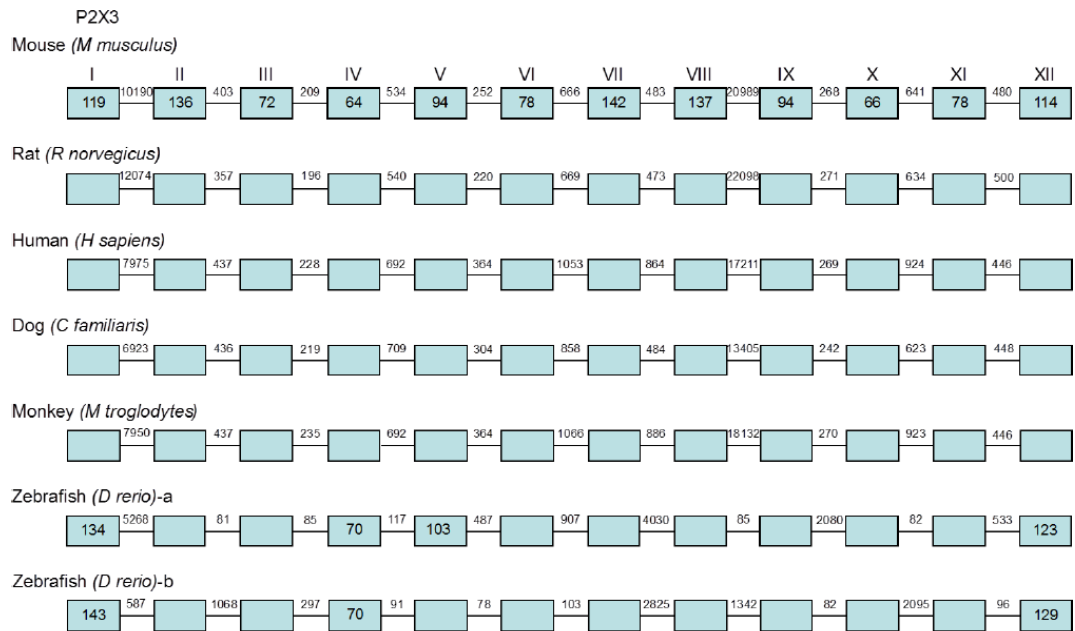
(a)



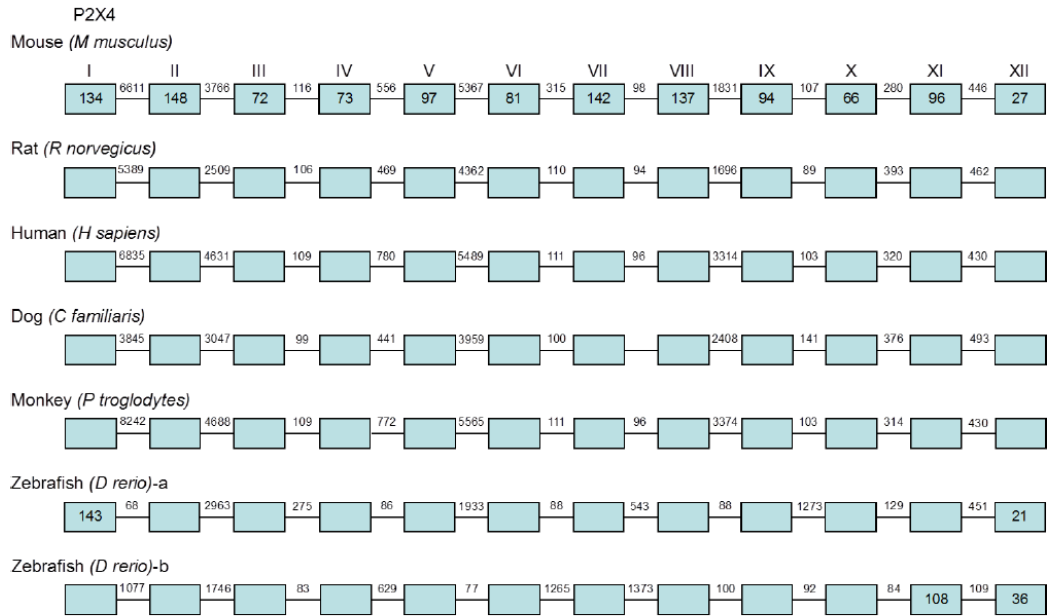
(b)



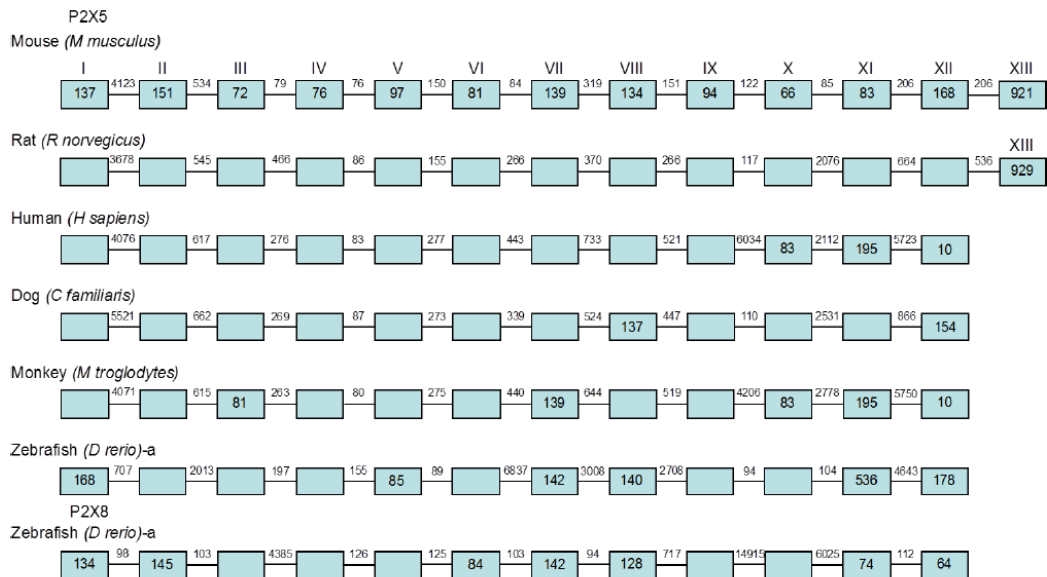
(c)



(d)



(e)



(f)

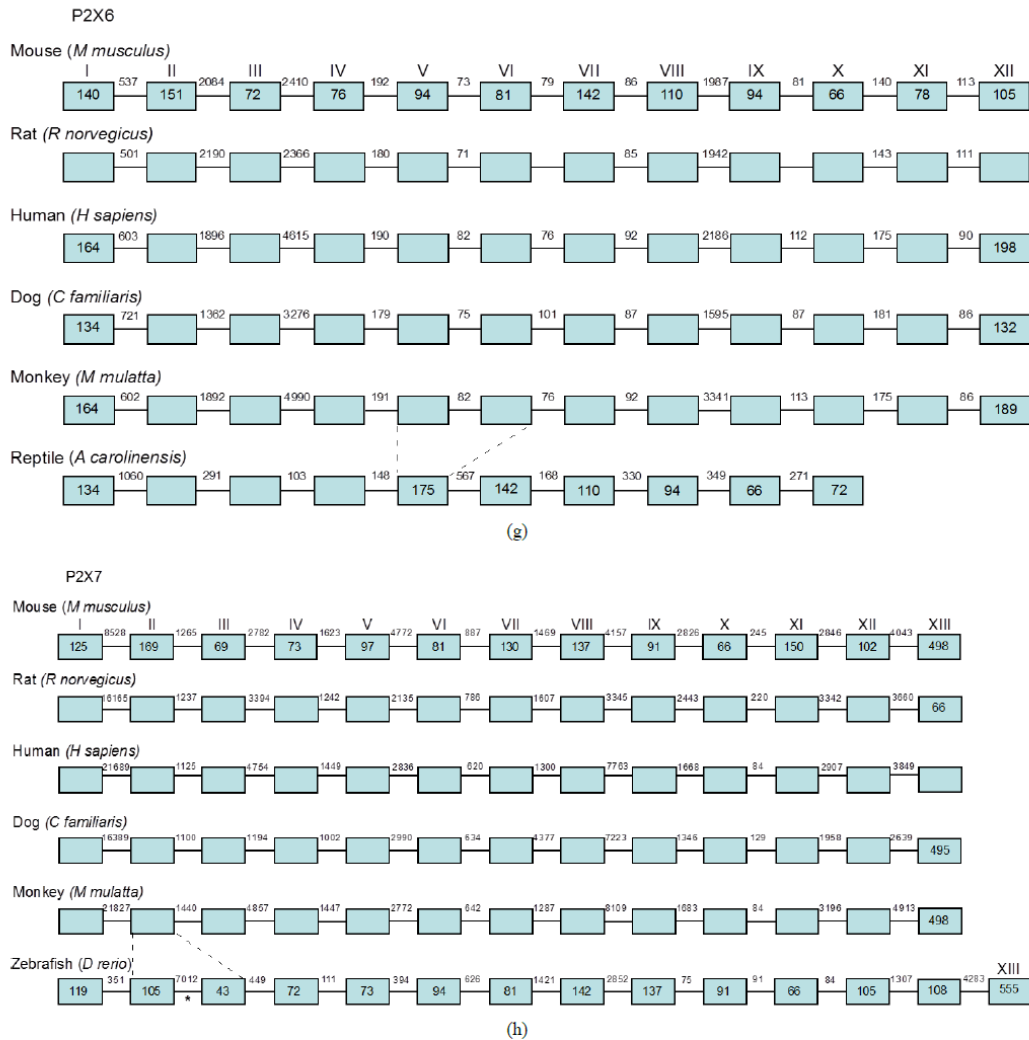


Figure 1. Schematic representation of the genomic organization of P2X receptors in several organisms. Exons are depicted as boxes with roman numbers on top, while introns are represented as solid lines. Numbers inside exons indicate the size in base pairs (bp) as well as number on top of the solid lines represent the intron size in bp. The first gene belongs to mouse in all cases and the lack of label below a given exon represents the conservation of size between homologous genes. (a) Genomic organization of the seven P2X subunits of mouse (*Mus musculus*); (b)-(h) Genomic organization of the P2X subunits compared between orthologous. When indicated, a dashed line points to exon fusion or exon separation between orthologous P2X genes.

Intron I is often referred to contain expression enhancers and other regulatory elements in mammals [30]-[32], this is the case of the purine nucleoside phosphorylase, where short portions of the intron 1 (around 170 bp) provided enhanced transcription in mammalian cell culture expression systems. In P2X orthologs (Figures 1(b)-(h)), intron I size and sequence it's also conserved, possibly pointing to unidentified regulatory elements in P2X genes.

3.2. Genomic Organization of P2X Orthologous Genes

To determine how P2X gene orthologous have been conserved in evolution among species, we analyzed the ge-

nomous organization of the seven P2X subunits of different mammalian species, including mouse (musP2X), rat (rnoP2X), primates (mmuP2X for Macaculata and ptrP2X for Pan troglodytes), human (hsaP2X) and dog (cafP2X). Additionally, we included in this study the zebrafish (darP2X for *Dario rerio*) from the family Cyprinidae from the class Actinopterygii, as ancestral species of mammals. In zebrafish, nine P2X genes have been reported: P2X₁ to P2X₅ and P2X₇ which are orthologous to mammal subunits. Another two paralogous of P2X₃ and P2X₄ named P2X_{3b} and P2X_{4b}, and P2X₈ from which there are no reported orthologous in mammals [33]-[35]. From our phylogenetic tree, we could propose that P2X₈ is an orthologous gene to P2X₅, although further functional and pharmacological evidence could uncover more similarities between these two subunits.

When we analyzed the exon size of P2X gene orthologous, we found a high conservation among the different species of mammals, with some exceptions in the first and last exon (Figure 1). Also the zebrafish showed variability in the size of some exons compared to P2X subunits in mammals. On the contrary, intron size is variable in each ortholog of P2X subunits, however, the size of introns tend to be better conserved between the orthologous of a specific P2X subunit (Figures 1(a)-(h)). The zebrafish again presents the most variable arrangement of introns compared to the other species. For most introns, the identity percentage was not significant, but in rare events the identity rate was up to 70% (Table 3). Additionally, we discovered that P2X subunits have a conserved intron phase among musP2X paralogs (Table 4). Among orthologous, P2X genes conserve their intron phase as well, however, some changes do occur in P2X₅ and P2X₇, overall in the 3' region of introns (Table 4). Thus, we found that, in general, introns I, V, VI and VIII are in phase two, whereas exons II, III, VII, IX, X, XI and XII end up in phase zero. Only exon IV appear in phase one.

Some P2X paralogous are found in the same chromosome, like P2X₁ and P2X₅; P2X₂, P2X₄ and P2X₇ showing syntenic traits. On Figure 2 we show the blocks of syntenic P2X genes in mouse and human. The comparison with all the analyzed species is shown in Supplementary Table S1. The genes P2X₁ and P2X₅ conform a block of syntenic genes between mouse and human with opposite orientation. In a similar way, P2X₄ and P2X₇ are syntenic between all orthologs. In the zebrafish case, with two different P2X₄ genes, only P2X_{4b} keeps synteny with P2X₇ (Supplementary Table S1), and the P2X_{4a} is different than b and other orthologous regarding its chromosome location. We also found synteny for P2X₂ orthologs but these are located further away from P2X₄ and P2X₇ (Figure 2). In the case of P2X₃, the genes in positions 1, 2, -1 and -2 are conserved completely in the mouse and human, however, the orientation is inverted. In zebrafish, P2X_{3a} and b keep the same microsynteny than their orthologous. Genes that keep synteny with P2X₆ conserve order as well as orientation.

The ortholog genes P2X₁₋₇ are much conserved at the protein level, most of all between rat and mouse or between human and primate (Table 3). The identity percentages (Clustal W, Slow/Accurate, Gonnet) between rat and mouse range from 85% (P2X₇) to 99% (P2X₃). On a similar way, between human and primate, identities range between 97% (P2X₄) and 100% (P2X₇). The lowest identity percentages are found between mammals and zebrafish, with values around 50% in most cases. These results are in accordance with the phylogenetic tree (Figure 3) where rodents and primates are closer to each other and farthest from zebrafish.

It has been previously described that orthologous genes tend to conserve their intron position compared with non-orthologous genes, even when orthologous sequence identity is low [36]-[38]. We found low percentage of protein identity between P2X₁₋₇ from zebra fish regarding their respective mammalian orthologous. However, even when zebrafish is an evolutionary distant organism, it tended to conserve certain characteristics such as exon-intron organization and intron position with its mammalian counterparts, which makes evident the sharing of common ancestry in P2X evolution (Figure 3). The main difference between fish P2X genes and mammalian was centered in the size of introns, indicating some re-organization in exon-intron position after mammalian divergence.

In zebrafish, two paralogous genes for P2X₃ and P2X₄ have been reported with distinctive localization and genomic organization. Several lines of evidence have suggested that whole genome duplications occurred before the vertebrate/ascidian divergence [39] and, later on, in the lineage of teleostheus after tetrapod divergence where only one set of these duplicated genes were maintained [40]-[43]. This is supported by the existence of several duplicated segments in zebrafish chromosomes [44]. The two genes darP2X_{3a} and b seem to be the result of this duplication, since they are located in a cluster of duplicated genes found in different chromosomes and conserves synteny with their orthologous (Supplementary Table S1). In darP2X_{4a} and b there is no conservation of gene duplicates, each P2X₄ is located in a different chromosome near single copy genes. P2X_{4b} is close in position to darP2X₇, but that is not the case of darP2X_{4a}, therefore, it is possible that P2X_{4a} was origin-

Table 3. Global (needle) and local (water) alignments of P2X subunits gene orthologous in ebi's align software.

P2X ₁	Mouse vs X (needle/water)				
	Rat	Human	Dog	Monkey	Zebrafish
Intron I	69.9/69.8	44.8/43.9	45.7/45.3	44.4/43.6	42.3/41.1
II	66.5/67	52.8/53.2	54/54	57.7/59.2	2.8/42.1
III	87.6/87.6	58.2/55.5	52.4/49.3	55.7/54.3	6.9/39.7
IV	86.8/86.8	44/44.4	47.8/47.3	42.9/43.7	4/42.9
V	78.3/78.3	56.9/57.4	57/56.3	57.1/57	21.2/40.2
VI	78/78.7	50.7/50.2	54.5/53.2	52/50.5	28.8/36.8
VII	81.5/80.9	40.9/40	42.3/42.3	33.4/34	21.2/41.1
VIII	81.3/83.7	33/50.2	46.2/48.3	21.7/47.1	40.9/44.7
IX	79.8/79.5	60/58.6	54.3/52.2	58.8/59.1	14.7/45.8
X	86.3/86.5	63.4/62.2	54.9/53.1	62.7/58.4	38.8/36
XI	84.5/84.5	54.5/59.1	54.4/53.6	57/57.2	2.7/46.3

P2X ₂	Mouse vs X (needle/water)				
	Rat	Human	Dog	Monkey	Zebrafish
Intron I	89/90.3	21.3/46.5	54.8/57.8	22/53	3.6/30.5
II	92.9/94.8	55.9/55.9	48.7/49.6	56.8/57.8	7.2/48.1
III	87.7/89.9	53.9/50.9	51.1/48.1	51.9/50	43.5/48.6
IV	90/92.3	52.1/52.8	40.8/55.7	53.7/55.7	2.1/35.5
V	82.4/83.4	42.1/49.7	44.9/45.4	47.8/48.5	31/54.7
VI	67.6/68.9	43.1/49.1	36.2/44.4	43.9/49.5	37.5/51.8
VII	87.3/87.9	46/46.5	50.5/52.1	50.4/50.6	10.6/48.2
VIII	75.8/76.7	38.6/49.7	40.3/42.1	44.4/53.6	3.5/37.2
IX	75.5/76.6	47.2/47.2	37.4/52.6	49.3/49.3	33.6/43.2
X	82.8/84.7	57.6/58.8	55/57.1	58.5/61.2	21.1/46.5
XI	93.8/95.6	69.4/70.6	51.6/52.8	70.1/70.8	8/32.8

P2X ₃	Mouse vs X (needle/water)					
	Rat	Human	Dog	Monkey	Zebrafish _a	Zebrafish _b
Intron I	56.7/61	40.2/48.7	35.5/42.9	40.9/48.9	28.7/37.7	3.2/38.4
II	75.6/75.8	52.6/52.7	34.1/54.4	53.3/56.5	13.7/34.1	23.7/33.3
III	81.5/85.9	58.9/63.8	23.8/35.6	54.1/58.3	18.3/48.4	14.1/29.9
IV	79.7/80.4	49.1/49.4	44.6/44.6	49.6/49.9	13.2/46.2	8.8/36.7
V	78/78.3	48.9/48.9	44.5/49.2	48.9/48.9	26.4/40.1	20.5/47.8
VI	85.5/85.7	41.3/41.3	48.9/50.6	41.2/41.2	38.4/38.5	9.6/39.3
VII	80.1/80.3	36.2/52.5	45/47.4	38/48.6	7.9/38.8	10.8/40.1
VIII	68.7/68.8	43.7/48.2	39.4/43.7	40.8/44.8	0.3/58.2	4.1/38.6
IX	90.5/90.8	65.1/65.1	51.4/51.6	0.7/51.4	6.9/37.5	15.1/40
X	82.5/82.6	44.8/45.4	51.1/52.3	43.4/46.5	9.1/44.5	19.6/35.5
XI	74.6/74.8	55.5/55.5	50.2/50.2	55.1/55.1	40.9/44.5	12.5/45.5

P2X ₄	Mouse vs X (needle/water)					
	Rat	Human	Dog	Monkey	Zebrafish _a	Zebrafish _b
Intron I	55.2/54.6	40.4/46.1	34.5/43.7	41.2/40.3	0.7/46.7	9.7/43.3
II	41.1/41.6	29/40	42.7/44.1	30/39.7	43.3/43.5	39.7/41.6
III	71.2/71.2	63.9/63.6	55.6/56	59.3/55.8	25.7/39.6	41.9/48.4
IV	69.3/69.8	42.5/43.9	49.7/50.1	43.4/42.6	9.6/43.2	44.5/44.5
V	62.2/61.4	39.6/46.6	42.0/42.0	39.4/43.2	22.4/35.5	0.9/40.0
VI	24.9/30	23.9/45.9	22.9/37.4	22.7/46	16.6/39.6	17.3/33.6
VII	65.2/66.1	54.1/56.8	55.4/56.4	52.5/54.2	12.1/34.2	4.5/53.0

Continued

VIII	59.4/62.4	34.4/36.8	44.4/44.7	35.5/36.3	3.0/43.7	3.8/48.9
IX	72.5/72.5	51.9/49.6	46.6/48.6	53.2/51.9	6.0/42.7	50.5/50.9
X	54.7/54.6	50.3/50	45.6/45.9	52.9/50.1	27.3/39.3	18.0/42.6
XI	77.2/77	49.2/52.2	51.2/54.4	71.4/48.7	44.6/44.8	16.0/41.1
P2X ₅	Mouse vs X (needle/water)					
	Rat	Human	Dog	Monkey	Zebrafish	P2X8 Zebrafish
Intron I	65.1/64.5	47/44.4	42.3/41.3	44.5/44.5	10.5/40	1.8/37.4
II	83.5/83.3	57.7/56.8	53.6/51.9	56.9/56.9	16.7/68.4	13.0/36.0
III	69.6/69	30.3/52.7	29.3/38.1	29.4/54.4	17.8/40.9	8.0/34.0
IV	84.9/84.9	68.5/68.5	63.2/64.2	68.5/68.5	27/66.7	28.6/38.4
V	80.7/80.7	38.9/42.8	40.5/50.2	43/42.8	32/35.8	27.0/35.7
VI	84.9/84.9	41.7/42.8	54.1/50.7	40.7/41.3	2.4/31.9	22.8/34.1
VII	71.5/74.1	42.2/42.3	50.8/48.3	47.2/46.1	9.1/37.3	13.1/36.8
VIII	76.4/76	33.5/53	30.8/41.3	33.5/46.6	20.2/45.5	21.5/37.2
IX	87.1/87.1	1.3/50.3	2.7/56.7	2.1/45.5	2.8/36.4	0.6/37.7
X	70.4/70.2	43.1/41	4.4/39.6	33.3/39.7	2.5/59.8	22.4/38.9
XI	68.5/68.7	7.0/38	43.3/45.8	6.9/38.1	10.8/48.1	10.2/43.9
XII	83.1/83.1	NA	NA	NA	6.6/40.5	
P2X ₆	Mouse vs X (needle/water)					
	Rat	Human	Dog	Monkey	Zebrafish	Rat
Intron I	78.6/79.7	52.2/52.5	48/47.4	52.5/50.4	31.9/33.8	78.6/79.7
II	67.8/67.9	46.9/46.8	40.5/39.7	47.3/46.2	8.7/38	67.8/67.9
III	81/80.8	36.9/37.3	45.7/44.9	32.4/36.6	2.9/48.5	81/80.8
IV	77/78.9	66.5/64.1	50.5/57.1	62.6/58.7	50.5/46.4	77/78.9
V	86.5/86.5	55.1/54.7	46.7/56.6	53.4/54.1	-	86.5/86.5
VI	88.6/88.6	55.3/56.2	43.4/59.5	52.6/52.9	10/43	88.6/88.6
VII	86.2/86.2	65.6/70.5	64.1/65.1	64.9/70.5	29.1/50.6	86.2/86.2
VIII	63.8/63.6	46.6/42.3	44.8/42.8	39.4/38.6	10.2/42.8	63.8/63.6
IX	88.9/88.9	49.6/52.4	62.9/62.9	49.1/53.3	11.4/45.8	88.9/88.9
X	68.8/75.9	55.9/57.6	55.2/52.5	58.9/58.2	35.1/44.5	68.8/75.9
XI	81/80.5	57.3/72.2	53.8/54.7	55.6/70	-	81/80.5
P2X ₇	Mouse vs X (needle/water)					
	Rat	Human	Dog	Monkey	Zebrafish	Rat
Intron I	-	-	54.2/60.2	-	2.8/41.8	-
II	83.1/83.3	56.2/62.4	25.5/48.9	47.4/50.8	20.8/39.4	83.1/83.3
III	63.7/63.9	35.8/45.3	39/39.7	35.7/46.9	2.6/53.9	63.7/63.9
IV	54.7/54.7	41.6/41.6	32.2/42.6	45.6/42.2	14.1/36.6	54.7/54.7
V	40.7/41.4	35.2/35.9	42.9/42.9	34.2/35.1	23.4/36.9	40.7/41.4
VI	70.2/70.2	45.9/45.9	22.4/33.6	47.6/43.5	36.5/38.4	70.2/70.2
VII	68.7/69	46.6/46.6	38/38	49.4/46.2	30.8/39.4	68.7/69
VIII	59.2/59.2	20.2/40	27.3/44.9	28.5/44.4	1.3/46.2	59.2/59.2
IX	59/59	29.2/45.9	25/43.8	29.3/45.4	2.1/39.3	59/59
X	69/69	21.1/60.4	38.1/40.1	23.8/52.8	18.4/46.6	69/69
XI	50.8/53.5	43/40.8	40/40.1	37/34.9	28.9/34.5	50.8/53.5
XII	64.1/63.8	44.6/41.9	39.9/41.6	43.7/41.7	22.2/36.7	64.1/63.8

Table 4. Intron phase of P2X paralogous of mouse.

Intron #	Intron Phase (at the end of intron)						
	musP2X ₁	musP2X ₂	musP2X ₃	musP2X ₄	musP2X ₅	musP2X ₆	musP2X ₇
1	2	2	2	2	2/0 ^a	2	2
2	0	0	0	0	0	0	0
3	0	0	0	0	0	0	0
4	1	1	1	1	1	1	1
5	2	2	2	2	2	2	2
6	2	2	2	2	2	2	2
7	0	0	0	0	0	0	0
8	2	2	2	2	2	2	2
9	0	0	0	0	0	0	0
10	0	0	0	0	0/2 ^b	0	0/1 ^c
11	0	0	0	0	2	0	0/1 ^c
12					2		

^aPhase zero only in darP2X₅. ^bPhase two only in hsaP2X₅ and ptrP2X₅. Phase 1 in darP2X₇.

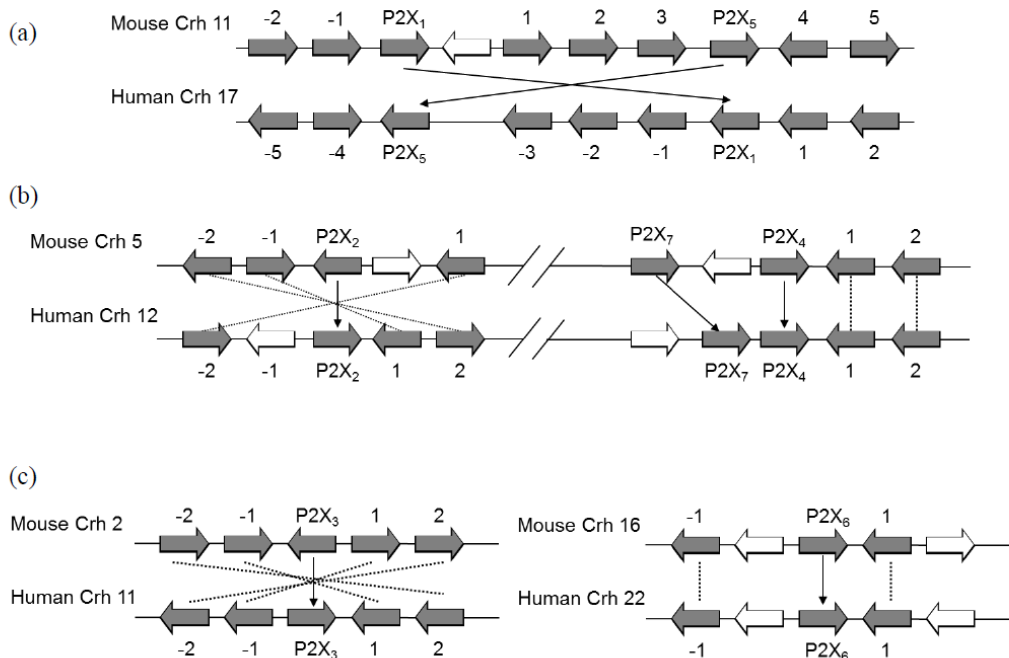


Figure 2. Microsynteny of P2X genes between mouse and human. The coding genes in chromosomes are depicted as filled arrows, while white filled arrows represent non-syntenic genes between mouse and human. The mouse was used as reference to catalog neighbor genes either upstream (negative numbers) or downstream (positive numbers) of the first P2X subunit found in the Watson DNA chain. Arrowhead lines represent the changes in P2X positions and dashed lines shows the changes in position of the neighbor genes. Gene Bank names for neighbor genes are shown in Supplementary Table S1. (a) Microsynteny of P2X₁ and P2X₅ genes. Schematic representation of the location of P2X₁ and P2X₅ in human and murine chromosomes respect to their chromosomal environment. Change in chromosome localization, sense of transcription and microsynteny of two genes for P2X₁ and five genes for P2X₅ can be observed; (b) Microsynteny of P2X₂, P2X₄ and P2X₇. Inversion of transcription sense and conservation of upstream genes -1 and -2 is shown, whereas genomic context is highly conserved for P2X₄ and P2X₇; (c) Microsynteny of P2X₃ and P2X₆. For P2X₃ inversion is observed in the whole chromosome context of the four neighbor genes. For P2X₆ genomic context is highly conserved for two genes on both sides.

nated in an independent duplication event explaining the lack of synteny in this gene.

We also analyzed the P2X orthologous intron phase to look for clues about the common ancestor of these genes as has been done elsewhere [45]. We found that intron phase is conserved in paralogous as well as in orthologous, with the zero phase as the most common, followed by phase two and phase one. Phase zero is the most common between mammalian orthologous and it's frequently found at the 3' region of a given gene [46]-[48]. Phase two is often referred as least common in gene arrangements; however P2X genes present this phase with a significant frequency. The implications of this phase conservation can be directly related to the allowance of functional variability. This is also correlated with the presence of phase zero in the conserved regions coding for transmembrane domains and C-terminus, which play significant roles in function and regulatory activity. Higher variability in exons coding for the extracellular domains could allow the evolution of regions affecting ligand affinity and gating.

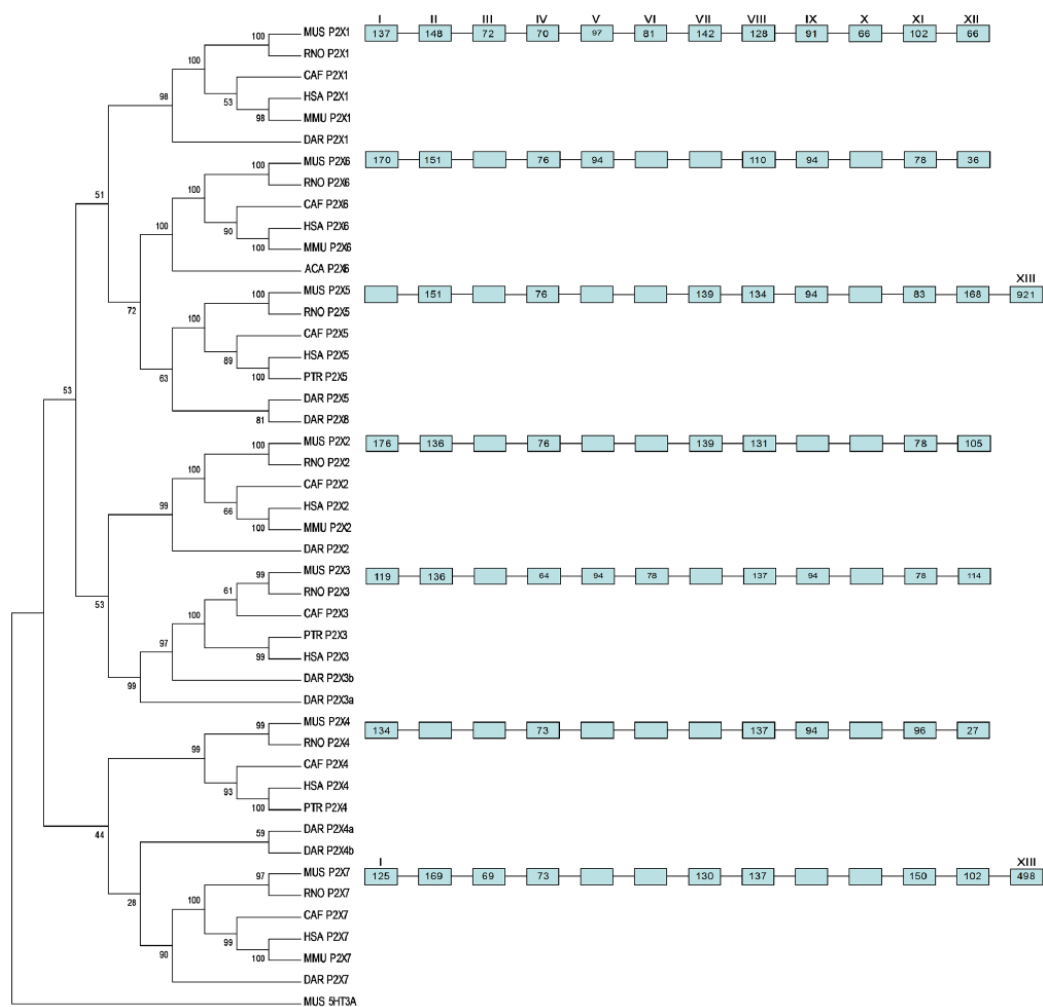


Figure 3. Phylogenetic tree representing P2X subunits from different organisms. *Mus musculus* (MUS), *Rattus norvegicus* (RNO), *Canis familiaris* (CAF), *Homo sapiens* (HSA), *Macaca mulatta* (MMU), *Danio rerio* (DAR), *Pan troglodytes* (PTR). 5HT3 receptor from mouse was used as external gene to perform the alignment using the MEGA software version 4.0 with the maximum Parsimony method (500 bootstrap). Numbers on the branches shows evolutionary distance represented as number of substitutions per residue. On the first branch of every clade the corresponding P2X subunit (1 to 7) gene is depicted.

In the next section, we describe particular characteristics of genomic organization for every P2X gene.

3.2.1. P2X₁

Mouse P2X₁ gene has a size of 16.05 Kb and mRNA of 1200 bp, which produces a protein of 399 aminoacids. The gen is organized in 12 exons and 11 introns. This organization is conserved among its mammals orthologous (rat, human, dog and primate) and differs with zebrafish organization, which has 13 exons and 12 introns (**Figure 1(b)**).

The size of P2X₁ exons is fully conserved in mammals, while conservations is sound only with exons III, VI, VII, IX and X of zebrafish (**Figure 1(b)**). An additional exon is present in darP2X₁ (exon XIII) with only 6 bp, from which only one aminoacid is coded together with the STOP codon.

P2X₁ introns are more divergent in size as well as in identity between the analyzed sequences. The first intron is the largest with >7400 bp in all the analyzed species. Using the Align algorithm (European Bioinformatics Institute) in its global (needle) and local (water) configuration we found identity values shown in **Table 3**. We showed that rat and mouse introns have the higher global identity (>66%) and intron IV has the highest unitary identity (87.6% in both needle/water modes). The zebrafish P2X₁ introns had the lower identity percentage (below 42.3% needle).

3.2.2. P2X₂

The P2X₂ gene of mouse is located in chromosome 5 and is characterized for being the shorter of mammal P2X genes (around 3 Kb, **Table 1**), mRNA without untranslated regions is 1248 bp long coding for a 416 aminoacid protein. P2X₂ gene was originally described by Brandle in 1997 with an organization of 11 exons and 10 introns, according to the NCBI reference P2X₂₋₁ (NM_053656). In previous work from our group we reported that P2X₂₋₂ isoform is actually the primary P2X₂ transcript and not the P2X₂₋₁ subunit as initially assumed. Based on this report we established the genomic arrangement of guinea pig P2X₂ as formed by 12 exons and 11 introns.

Since P2X₂₋₂ isoform is expressed in all mammals where splicing studies have been done (namely, mouse, rat and human), we have extrapolated the guinea pig model to the rest of species and confronted it with the genomic arrangement of zebrafish P2X₂ (**Figure 1(c)**). The addition of an exon in this 12 exon-11 intron arrangement is given by the separation of the last exon into two new exons (XI and XII) separated by an intron. To identify the donor and acceptor sites in this intron we use Net Gene2 algorithm (www.cbs.dtu.dk/services/NetGene2/) with all the analyzed P2X₂ gene sequences. In all genes we found a donor site with high confidence level at the beginning of the site where intron 11 is located. In the same way, we found an acceptor site in the same intron in human and guinea pig. For mouse and rat the site could be easily identified using the GT/AG rule. These sites support the existence of the intron 11 between exons XI and XII with a size of 91 or 206 bp, depending on the species (**Figure 1(c)**).

Phylogenetically, P2X₂ is closer to P2X₃ (**Figure 3**), which is reflected also in the conservation of the genomic arrangement of 12 exons and 11 introns between these paralogous. The same order is maintained among the orthologous of P2X₂, even with the more distant zebrafish (**Figure 1(c)**). With the exception of exons I, IX and XII, all exons conserve their size, including exon XI of 78 bp shared entirely by P2X₃ (**Figure 2**).

On its part, P2X₂ introns are less conserved and are characterized for their small size, however, introns size in zebrafish P2X₂ are variable, ranging from small (3, 5 and 9 of 81, 76 and 81 respectively) to large introns (intron 8 is 3027 bp). This contrasts with mammalian P2X₂ genes with no intron larger than 450 bp. In nucleotide sequence, the better conserved, both globally and locally regarding mouse are rat's introns 1 (89/90.3), intron 2 (92.9/94.8), intron 4 (90/92.3) and intron 11 (93.8/95.6). With the rest of orthologous the identity are equal or lower than 70%.

We have suggested that genomic organization of P2X₂ in mammals is composed of 12 exons and 11 introns, such as it's been displayed in Ensembl and fast DB databases. This model is based in the evidence that P2X₂₋₂ or P2X_{2b} is the only mammal homologous to zebrafish P2X₂, which have P2X duplications rather than reductions in gene number. Additionally we observed that P2X₂₋₂ genomic arrangement is conserved between mammalian orthologous and the distant zebrafish. In the same way, this isoform is more close to the paralogous P2X₃, indicating our proposed genomic organization has a better evolutionary meaning than the previously proposed model.

We also observed that mammalian P2X₂ size is smaller than zebrafish P2X₂, showing a large variation in in-

tron size. This suggests that P2X₂ went over a shortening of introns that could have conferred a regulatory function in a similar way to some constitutive genes [22] [24]. All the intron phases are conserved in P2X₂ orthologous, suggesting that no major genomic re-arrangements have occurred. This is supported by functional evidence of our laboratory, where P2X₂ expression is sustained in myenteric neurons during embryonic development and to adulthood, implying the functionality of the subunit in a range of physiological events.

3.2.3. P2X₃

The murine P2X₃ receptor has a genomic size of 39.2 Kb and a mRNA of 1.4 Kb, coding for a 397 aminoacids protein. Its chromosomal localization is shown in **Table 1**. The genomic organization of P2X₃ is shown in Fig. 1D with an arrangement of 12 exons and 11 introns, which is conserved among orthologous.

The aminoacidic identities of P2X₃ between mouse and its orthologous were the highest of all P2X genes (higher than 93%). From the two P2X₃ genes in zebrafish, darP2X₃b had the highest identity with mammalian P2X₃ (68% with Clustal W), while darP2X₃a had 57% identity. When we compared P2X₃a with P2X₃b, we found 58% of identity. These results are in agreement with the phylogenetic tree shown in **Figure 3**, where darP2X₃b is closer to mammalian P2X₃ genes.

Figure 1(d) shows the high conservation between the mammalian orthologous, only some differences appear in exons I, IV, V and XII of zebrafish P2X₃ compared to mouse. Intron sequences between mouse and rat are highly identical; in intron 9 the conservation is 90.5/90.8% needle/water, intron 11 has a 74.6% needle identity, the same intron has up to 55.5% global identity compared to other mammals. As expected, the zebrafish has shorter and less conserved introns compared to other P2X₃ mammalian genes.

The evidence on P2X₃ suggests, together with other P2X subunits sequences, that zebrafish had a common ancestor with mammals. The divergence of these two lineages can be inferred with the accumulation of genetic material in mammal introns. In mammals, intron 8 has a larger size than zebrafish sequences. When we performed a PSI-BLAST analysis in this intron, we observed the presence of several elements similar to dSpmZea transposons, suggesting the increase in mammalian intronic sequences could be due to transposon insertion [37] [49] [50]. The phylogenetic analysis shows darP2X₃a isoform diverging before the separation of mammalian clade (**Figure 3**), which leads us to propose that mammalian P2X₃ sequences are derived from darP2X₃b found in the zebrafish ancestor.

3.2.4. P2X₄

Mouse P2X₄ receptor is located close to P2X₇ in chromosome 5, it has a 21.488 Kb size and mRNA of 1,995 bp, coding for a protein of 388 aminoacids (see **Table 1** and **Figure 2**). Analyzing genomic organization of P2X₄ (**Figure 1(e)**) we can see it's comprised of 12 exons and 11 introns. The phylogenetic tree shows it closer to P2X₇, however they do not share the same exon-intron arrangement. In zebrafish, P2X₄ paralogous (a and b) are kept in the same clade in the tree and have an identity of 57% between both proteins (**Figure 3**). Comparing musP2X₄ with the two zebrafish isoforms darP2X₄a and darP2X₄b using Clustal W, we encountered identities of 58% and 52% respectively (**Table 5**). Exon size is completely conserved among P2X₄ orthologous in mammals (**Figure 1(e)**). In zebrafish, the two P2X₄ genes conserve exon size compared to mouse; darP2X₄a differs only in the first and last exon, whilst darP2X₄b differs in the last two.

The size of introns is variable among P2X₄ orthologous; with sizes ranging from 99bp to 8 Kb. Introns 1 and 5 are the largest while intron 7 and 9 are the smallest. Comparing intron identity between orthologous we found the highest identities again between mouse and rat, particularly in introns 3, 4, 9 and 11, with 71/71%, 69/70%, 72/72% and 77/77% needle/water identity respectively (**Table 3**).

We observed that even when darP2X₄a has a higher global identity with their orthologous than darP2X₄b, synteny occurs with P2X₄b and P2X₇ suggesting that P2X₄b was prior to genome duplication events that happened in zebrafish after mammalian divergence and therefore, originated the mammalian P2X₄ genes.

3.2.5. P2X₅

In mouse, P2X₅ receptor is located in chromosome 11 and has a size of 12.16 Kb with a mRNA of 2.293 Kb after the editing of their 13 exons and 12 introns. The P2X₅ subunit has 455 aminoacids. The genomic organization of mouse P2X₅ is quite unique, since it is conserved with the rat, but it's different to the other mammals analyzed, which present an organization of 12 exons and 11 introns.

Looking the phylogenetic tree on **Figure 2**, we can see that darP2X₅ is grouped in the same clade than P2X₅,

Table 5. Percent identity of mouse P2X orthologous genes (clustal W).

P2X ₁	MUS	RNO	HSA	MMU	CAF	DAR		
MUS	***	97.5	89.5	90	89.2	55.2		
RNO		***	89	89.5	88.5	54.9		
HSA		12	***	97.5	90.7	54.4		
MMU				***	90.7	54.9		
CAF					***	56.2		
DAR						***		
P2X ₂	MUS	RNO	HSA	MMU	CAF	DAR		
MUS	***	97.5	89.5	90	89.2	55.2		
RNO		***	89	89.5	88.5	54.9		
HSA		12	***	97.5	90.7	54.4		
MMU				***	90.7	54.9		
CAF					***	56.2		
DAR						***		
P2X ₃	MUS	RNO	HSA	PTR	CAF	DARa	DARb	
MUS	***	99	93.7	94	94.5	57.5	68	
RNO		***	93.7	94	94.5	57.2	68	
HSA			***	99.7	94.7	58	68.3	
PTR				***	95	58	68.3	
CAF					***	57.2	67.8	
DARa						***	58.2	
DARb							***	
P2X ₄	MUS	RNO	HSA	PTR	CAF	DARa	DARb	
MUS	***	94.6	87.4	87.4	86.1	57.8	51.7	
RNO		***	87.1	87.1	85.3	59.3	51.9	
HSA			***	100	89.9	58.3	53.2	
PTR				***	89.9	58.3	53.2	
CAF					***	56.5	52.2	
DARa						***	57.1	
DARb							***	
P2X ₅	MUS	RNO	HSA	PTR	CAF	DAR	darP2X8	
MUS	***	94.7	69.2	69	70	50.2	43.5	
RNO		***	69	68.8	70.2	49.6	44	
HSA			***	99.5	76.8	48.9	44	
PTR				***	77	48.9	44	
CAF					***	53	46.2	
DAR						***	51	
P2X ₆	MUS	RNO	HSA	MMU	CAF	DAR		
MUS	***	94.7	69.2	69	70	60.2		
RNO		***	69	68.8	70.2	60.2		
HSA			***	99.5	76.8	58.5		
MMU				***	77	58		
CAF					***	59.6		
DAR						***		
P2X ₇	MUS	RNO	HSA	MMU	CAF	DAR		
MUS	***	85	80.8	80.5	76.6	45.2		
RNO		***	80.3	80.2	76.4	44.5		
HSA			***	97.1	86.2	46.2		
MMU				***	85.5	46.2		
CAF					***	46.4		
DAR						***		

suggesting an evolutionary relationship between these two sequences. The gene darP2X₈ has 44% identity with musP2X₅, which is the same identity of darP2X₅. On the other hand the tree shows P2X₅ close to P2X₆ but their genomic organization is not conserved.

There is conservation in exon size between mammalian P2X₅ genes, overall among exons I to V (**Figure 1(g)**). With zebrafish orthologous P2X₅ and P2X₈ the size of exons is more variable. Intron sequence is the most similar between rat and mice with introns 3, 9 and 11, which have global identities superior to 70%.

As shown in **Figure 1(g)**, introns 2, 7, 8 and 11 are longer in zebrafish than in the other organisms analyzed, thus it is probable that loss of genetic material could give some advantage in P2X₅ expression in mammals [51] [52].

The receptor darP2X₈ is grouped with P2X₅ in the phylogenetic tree; therefore we compared the nucleotide sequence and observed certain similarity between them. For example, the highest identity of 66.3% occurred for Exon VI (needle, data not shown). This is evidence of distant divergence between P2X₅ and P2X₈. However this is the only case where zebrafish has the same intron phase than the mammalian P2X₅ genes. This is additional evidence to the previously suggested evolutionary relationship between P2X₅ and P2X₈ in chicken (*Gallus gallus*) [53].

3.2.6. P2X₆

The murine P2X₆ gene has a size of 10.13 Kb and a mRNA of 1170 bp, generating a product of 389 aminoacids. The P2X₆ is organized in 12 exons and 11 introns; this organization is conserved among mammalian orthologous. Since zebrafish seems to lack P2X₆, we choose a reptile (*Anolis carolinensis*) as a possible distant species to compare gene sequences. In the case of *A. carolinensis* P2X₆ gene (acaP2X₆), its organization has 11 exons and 10 introns (**Figure 1(g)**).

Comparing exon size of mouse P2X₆ with its orthologous we observed that is conserved in all the mammalian species, with the exception of the first and last exons, as with other P2X analyzed. However, exon V of acaP2X₆ is 175 bp long, which is equivalent to the sum of the individual size of exons V (94 bp) and VI (81 bp) from mouse P2X₆. Reptilian exons from VI to X conserve the size with exons VII to XI of musP2X₆, respectively.

Introns present the higher divergence in size and identity among the analyzed sequences. Introns 2, 3 and 8 are the largest (more than 1200 bp) in mammals; while in reptile intron 1 had the larger size with 1060 bp (**Figure 1(g)**). Comparing intron sequence of mouse P2X₆ against its orthologs, as observed in **Table 3**, we found that rat and mouse have the highest identity (above 63%), with intron 9 the highest in score (88.9/88.9% needle/water). Introns from reptile P2X₆ had the lower identity percentage (below 50.5%).

Our analysis of P2X₆ sequences between mammals and reptile suggest that P2X genes were present in a common ancestor. We encountered the accumulation of genetic material in the case of some mammalian P2X₆ introns, including the presence of an intron between exons V and VI of mammals that is not observed in reptile. Mammalian exons V and VI match exactly in size with reptilian exon V, with identities of 60.8 and 73.2% respectively when aligned locally (data not shown). This explains the presence of only 11 exons in the reptile compared to the 12 exons in mammalian P2X₆. The presence of the same genetic structure in all of mammals points that the intron present between exons V and VI was acquired more recently after reptilian and mammalian divergence through insertion. It has been proposed recently that the increased number of introns in an organism is related to less efficient expression. The insertion of this intron can contribute, along with other multiple regulatory mechanisms, to the in vivo behavior of P2X₆ receptors.

3.2.7. P2X₇

The murine gene coding for P2X₇ is the largest of the P2X family. In mice it has 37.2 Kb with a transcript of 1785 bp, giving a protein of 595 aminoacids. The gene organization of P2X₇ consists of 13 exons and 12 introns in mammals and 14 exons and 13 introns in zebrafish (dar P2X₇, **Figure 1(h)**). This genomic organization is different to what is seen for other P2X genes (**Figure 1(a)**).

The P2X₇ subunit is notable for its longer C-terminus, with 230 aminoacids for mouse, compared to the shorter C-terminus of musP2X₆ with only 25 aminoacids and musP2X₅ with 94 aminoacids (second largest). Protein size is identical in the five mammalian species (**Table 1**), which is also reflected in the high conservation of the exon size. The only differences we found were in exons VII and XII of dog (**Figure 1(h)**).

The introns of P2X₇ are in general long, overall intron 1 which has more than 21000 bp in both human and mouse, contrasting with intron 10 with 84 to 245 bp. Intron 2 is very well conserved among species, with identities as high as 83% local/global between rat and mouse. Intron phase is conserved among mammalian species,

however, darP2X₇ (fish) have a shift in phases due to an insertion of an intron in exon II. Also the last three introns of the zebrafish uses phase one instead the phase zero of mammals.

The main difference between the P2X₇ of mammals is their large size compared to the one of zebrafish (Table 1). Also exon-intron organization of the zebrafish is different to the mammalian genes, since it consists of a large intron of 7012 bp with a translated sequence corresponding to the reverse transcriptase of a retrotransposon (Accession No.: XP_694080). This evidence suggests the insertion of the intronic sequence in exon 2 after the divergence of mammalian and fish lineages, generating the new exons II and III in darP2X₇ only. This suggests an evolutionary story where several insertions occurred in the lineage of zebrafish, elongating the introns of P2X₇ and conserved until know possibly to an advantage in expression regulation.

4. Concluding Remarks

The evolutionary origin of P2X receptors is still unclear; however, ancestral organisms diverging as far as 1 billion years ago have a single P2X receptor that has pharmacological and biophysical properties that resemble those of the seven P2X subunits in vertebrates [14] [17] [18] [54] [55]. As we have shown in this work, there is a high conservation of the gene structure among P2X receptors in the different organisms analyzed, even in the distant species of fish and reptile. This is additional evidence pairs with previous reports proposing that a single gene in a common ancestor very recently originates the current diversity of P2X subunits in vertebrates [14] [17]. After vertebrate divergence, P2X genes underwent duplications, gain of intron sequences and exon rearrangements that give the seven genes coding for P2X subunits a complexity underlying an important portion of the purinergic signaling in mammals.

Our phylogenetic tree shows P2X₄ and P2X₇ as members of a more related clade. This is in agreement with previous hypothesis suggesting their origin from gene duplication [56]. Their joint evolution can be driven by the selective pressure generated by their functional role in the central nervous system, where these two subunits are mainly responsible for the activation of the inflammasome after injury [57]. In a similar way, the localization of P2X₂ and P2X₃ in a clade with a recent common ancestor correlates with their high rate of appearance as heteromers in sensory neurons [9]. More importantly, an increasing amount of works have proven that P2X represents important therapeutic targets in pathologies as important as chronic pain in cancer and inflammation [58] [59]. With only few selective antagonists available [19], new strategies such as gene therapy can be the more effective choice when it comes to selectively regulate heteromeric P2X activation in cells [60]. In this work we provide a comprehensive depiction of the genomic organization of P2X receptors in the major model species of mammals. We expect our results will help to better understand phenomena at the transcription level such as splicing variants of P2X receptors and also to provide easy to access reference about the differences of P2X subunits at the nucleotide level, thus allowing to better design future strategies in basic science and therapeutics of P2X physiology.

Acknowledgements

This work is funded by the National Council of Science and Technology in Mexico (CONACYT). We thank Dr. Yair Cárdenas-Conejo for his valuable inputs and comments to this work.

References

- [1] North, R.A. (2002) Molecular physiology of P2X receptors. *Physiological Reviews*, **82** 1013-1067. <http://dx.doi.org/10.1152/physrev.00015.2002>
- [2] Cockayne, D.A., Dunn, P.M., Zhong, Y., Rong, W., Hamilton, S.G., Knight, G.E., Ruan, H.Z., Ma, B., Yip, P., Nunn, P., McMahon, S.B., Burnstock, G. and Ford, A.P. (2005) P2X₂ Knockout Mice and P2X₂/P2X₃ Double Knockout Mice Reveal a Role for the P2X₂ Receptor Subunit in Mediating Multiple Sensory Effects of ATP. *The Journal of Physiology*, **567**, 621-639. <http://dx.doi.org/10.1113/jphysiol.2005.088435>
- [3] Burnstock, G. (2007) Physiology and Pathophysiology of Purinergic Neurotransmission. *Physiological Reviews*, **87**, 659-797. <http://dx.doi.org/10.1152/physrev.00043.2006>
- [4] Coutinho-Silva, R., Knight, G.E. and Burnstock, G. (2005) Impairment of the Splenic Immune System in P2X₂/P2X₃ Knockout Mice. *Immunobiology*, **209**, 661-668. <http://dx.doi.org/10.1016/j.imbio.2004.09.007>
- [5] Huang, L.C., Greenwood, D., Thome, P.R. and Housley, G.D. (2005) Developmental Regulation of Neuron-Specific P2X₃ Receptor Expression in the Rat Cochlea. *Journal of Comparative Neurology*, **484**, 133-143.

- <http://dx.doi.org/10.1002/cne.20442>
- [6] Torres, G.E., Egan, T.M. and Voigt, M.M. (1999) Hetero-Oligomeric Assembly of P2X Receptor Subunits. Specificities Exist with Regard to Possible Partners. *The Journal of Biological Chemistry*, **274**, 6653-6659. <http://dx.doi.org/10.1074/jbc.274.10.6653>
- [7] Valera, S., Hussy, N., Evans, R.J., Adami, N., North, R.A., Surprenant, A. and Buell, G. (1994) A New Class of Ligand-Gated Ion Channel Defined by P2X Receptor for Extracellular ATP. *Nature*, **371**, 516-519. <http://dx.doi.org/10.1038/371516a0>
- [8] Surprenant, A., Buell, G. and North, R.A. (1995) P_{2X} Receptors Bring New Structure to Ligand-Gated Ion Channels. *Trends in Neurosciences*, **18**, 224-229. [http://dx.doi.org/10.1016/0166-2236\(95\)93907-F](http://dx.doi.org/10.1016/0166-2236(95)93907-F)
- [9] Xiang, Z. and Burnstock, G. (2004) P2X₂ and P2X₃ Purinoceptors in the Rat Enteric Nervous System. *Histochemistry and Cell Biology*, **121**, 169-179. <http://dx.doi.org/10.1007/s00418-004-0620-1>
- [10] Chen, C.C., Akopian, A.N., Sivilotti, L., Colquhoun, D., Burnstock, G. and Wood, J.N. (1995) A P2X Purinoceptor Expressed by a Subset of Sensory Neurons. *Nature*, **377**, 428-431. <http://dx.doi.org/10.1038/377428a0>
- [11] Garcia-Guzman, M., Stuhmer, W. and Soto, F. (1997) Molecular Characterization and Pharmacological Properties of the Human P2X₃ Purinoceptor. *Molecular Brain Research*, **47**, 59-66. [http://dx.doi.org/10.1016/S0169-328X\(97\)00036-3](http://dx.doi.org/10.1016/S0169-328X(97)00036-3)
- [12] Ren, J., Bian, X., DeVries, M., Schnegelsberg, B., Cockayne, D.A., Ford, A.P. and Galligan, J.J. (2003) P2X₂ Subunits Contribute to Fast Synaptic Excitation in Myenteric Neurons of the Mouse Small Intestine. *The Journal of Physiology*, **552**, 809-821. <http://dx.doi.org/10.1113/jphysiol.2003.047944>
- [13] Ruan, H.Z. and Burnstock, G. (2005) The Distribution of P2X₅ Purinergic Receptors in the Enteric Nervous System of Mouse. *Cell and Tissue Research*, **319**, 191-200. <http://dx.doi.org/10.1007/s00441-004-1002-7>
- [14] Fountain, S.J. and Burnstock, G. (2009) An Evolutionary History of P2X Receptors. *Purinergic Signalling*, **5**, 269-272. <http://dx.doi.org/10.1007/s11302-008-9127-x>
- [15] Burnstock, G. and Verkhratsky, A. (2009) Evolutionary Origins of the Purinergic Signalling System. *Acta Physiologica*, **195**, 415-447. <http://dx.doi.org/10.1111/j.1748-1716.2009.01957.x>
- [16] Trams, E.G. (1981) On the Evolution of Neurochemical Transmission. *Differentiation*, **19**, 125-133. <http://dx.doi.org/10.1111/j.1432-0436.1981.tb01140.x>
- [17] Bavan, S., Straub, V.A., Blaxter, M.L. and Ennion, S.J. (2009) A P2X Receptor from the Tardigrade Species *Hypsibius dujardini* with Fast Kinetics and Sensitivity to Zinc and Copper. *BMC Evolutionary Biology*, **9**, 17. <http://dx.doi.org/10.1186/1471-2148-9-17>
- [18] Agboh, K.C., Webb, T.E., Evans, R.J. and Ennion, S.J. (2004) Functional Characterization of a P2X Receptor from *Schistosoma mansoni*. *The Journal of Biological Chemistry*, **279**, 41650-41657. <http://dx.doi.org/10.1074/jbc.M408203200>
- [19] Muller, C.E. (2015) Medicinal Chemistry of P2X Receptors: Allosteric Modulators. *Current Medicinal Chemistry*, **22**, 929-941. <http://dx.doi.org/10.2174/0929867322666141210155610>
- [20] Rodriguez-Kessler, M., Delgado-Sanchez, P., Rodriguez-Kessler, G.T., Moriguchi, T. and Jimenez-Bremont, J.F. (2010) Genomic Organization of Plant Aminopropyl Transferases. *Plant Physiology and Biochemistry*, **48**, 574-590. <http://dx.doi.org/10.1016/j.plaphy.2010.03.004>
- [21] Li, M., Chang, T.H., Silberberg, S.D. and Swartz, K.J. (2008) Gating the Pore of P2X Receptor Channels. *Nature Neuroscience*, **11**, 883-887. <http://dx.doi.org/10.1038/nn.2151>
- [22] Castillo-Davis, C.I., Mekhedov, S.L., Hartl, D.L., Koonin, E.V. and Kondrashov, F.A. (2002) Selection for Short Introns in Highly Expressed Genes. *Nature Genetics*, **31**, 415-418. <http://dx.doi.org/10.1038/ng940>
- [23] Eisenberg, E. and Levanon, E.Y. (2003) Human Housekeeping Genes Are Compact. *Trends in Genetics*, **19**, 362-365. [http://dx.doi.org/10.1016/S0168-9525\(03\)00140-9](http://dx.doi.org/10.1016/S0168-9525(03)00140-9)
- [24] Rao, Y.S., Wang, Z.F., Chai, X.W., Wu, G.Z., Zhou, M., Nie, Q.H. and Zhang, X.Q. (2010) Selection for the Compactness of Highly Expressed Genes in *Gallus gallus*. *Biology Direct*, **5**, 35. <http://dx.doi.org/10.1186/1745-6150-5-35>
- [25] Linan-Rico, A., Jaramillo-Polanco, J., Espinosa-Luna, R., Jimenez-Bremont, J.F., Linan-Rico, L., Montano, L.M. and Barajas-Lopez, C. (2012) Retention of a New-Defined Intron Changes Pharmacology and Kinetics of the Full-Length P2X₂ Receptor Found in Myenteric Neurons of the Guinea Pig. *Neuropharmacology*, **63**, 394-404. <http://dx.doi.org/10.1016/j.neuropharm.2012.04.002>
- [26] Brosenitsch, T.A., Adachi, T., Lipski, J., Housley, G.D. and Funk, G.D. (2005) Developmental Downregulation of P2X₃ Receptors in Motoneurons of the Compact Formation of the Nucleus Ambiguus. *European Journal of Neuroscience*, **22**, 809-824. <http://dx.doi.org/10.1111/j.1460-9568.2005.04261.x>

- [27] Ruan, H.Z., Moules, E. and Burnstock, G. (2004) Changes in P2X₃ Purinoceptors in Sensory Ganglia of the Mouse during Embryonic and Postnatal Development. *Histochemistry and Cell Biology*, **122**, 539-551. <http://dx.doi.org/10.1007/s00418-004-0714-9>
- [28] Xiang, Z. and Burnstock, G. (2004) Development of Nerves Expressing P2X₃ Receptors in the Myenteric Plexus of Rat Stomach. *Histochemistry and Cell Biology*, **122**, 111-119. <http://dx.doi.org/10.1007/s00418-004-0680-2>
- [29] Loera-Valencia, R., Jimenez-Vargas, N.N., Villalobos, E.C., Juarez, E.H., Lomas-Ramos, T.L., Espinosa-Luna, R., Montano, L.M., Huizinga, J.D. and Barajas-Lopez, C. (2014) Expression of P2X₃ and P2X₂ Myenteric Receptors Varies during the Intestinal Postnatal Development in the Guinea Pig. *Cellular and Molecular Neurobiology*, **34**, 727-736. <http://dx.doi.org/10.1007/s10571-014-0055-8>
- [30] Majewski, J. and Ott, J. (2002) Distribution and Characterization of Regulatory Elements in the Human Genome. *Genome Research*, **12**, 1827-1836. <http://dx.doi.org/10.1101/gr.606402>
- [31] Kalari, K.R., Casavant, M., Bair, T.B., Keen, H.L., Comeron, J.M., Casavant, T.L. and Scheetz, T.E. (2006) First Exons and Introns—A Survey of GC Content and Gene Structure in the Human Genome. *In Silico Biology*, **6**, 237-242.
- [32] Zhu, L., Zhang, Y., Zhang, W., Yang, S., Chen, J.Q. and Tian, D. (2009) Patterns of Exon-Intron Architecture Variation of Genes in Eukaryotic Genomes. *BMC Genomics*, **10**, 47. <http://dx.doi.org/10.1186/1471-2164-10-47>
- [33] Egan, T.M., Cox, J.A. and Voigt, M.M. (2000) Molecular Cloning and Functional Characterization of the Zebrafish ATP-Gated Ionotropic Receptor P2X₃ Subunit. *FEBS Letters*, **475**, 287-290. [http://dx.doi.org/10.1016/S0014-5793\(00\)01685-9](http://dx.doi.org/10.1016/S0014-5793(00)01685-9)
- [34] Diaz-Hernandez, M., Cox, J.A., Migita, K., Haines, W., Egan, T.M. and Voigt, M.M. (2002) Cloning and Characterization of Two Novel Zebrafish P2X Receptor Subunits. *Biochemical and Biophysical Research Communications*, **295**, 849-853. [http://dx.doi.org/10.1016/S0006-291X\(02\)00760-X](http://dx.doi.org/10.1016/S0006-291X(02)00760-X)
- [35] Kucenas, S., Li, Z., Cox, J.A., Egan, T.M. and Voigt, M.M. (2003) Molecular Characterization of the Zebrafish P2X Receptor Subunit Gene Family. *Neuroscience*, **121**, 935-945. [http://dx.doi.org/10.1016/S0306-4522\(03\)00566-9](http://dx.doi.org/10.1016/S0306-4522(03)00566-9)
- [36] Babenko, V.N., Rogozin, I.B., Mekhedov, S.L. and Koonin, E.V. (2004) Prevalence of Intron Gain Over Intron Loss in the Evolution of Paralogous Gene Families. *Nucleic Acids Research*, **32**, 3724-3733. <http://dx.doi.org/10.1093/nar/gkh686>
- [37] Carmel, L., Rogozin, I.B., Wolf, Y.I. and Koonin, E.V. (2007) Patterns of Intron Gain and Conservation in Eukaryotic Genes. *BMC Evolutionary Biology*, **7**, 192. <http://dx.doi.org/10.1186/1471-2148-7-192>
- [38] Rogozin, I.B., Wolf, Y.I., Sorokin, A.V., Mirkin, B.G. and Koonin, E.V. (2003) Remarkable Interkingdom Conservation of Intron Positions and Massive, Lineage-Specific Intron Loss and Gain in Eukaryotic Evolution. *Current Biology*, **13**, 1512-1517. [http://dx.doi.org/10.1016/S0960-9822\(03\)00558-X](http://dx.doi.org/10.1016/S0960-9822(03)00558-X)
- [39] Okamura, Y., Nishino, A., Murata, Y., Nakajo, K., Iwasaki, H., Ohtsuka, Y., Tanaka-Kunishima, M., Takahashi, N., Hara, Y., Yoshida, T., Nishida, M., Okado, H., Watari, H., Meinertzhagen, I.A., Satoh, N., Takahashi, K., Satou, Y., Okada, Y. and Mori, Y. (2005) Comprehensive Analysis of the Ascidian Genome Reveals Novel Insights into the Molecular Evolution of Ion Channel Genes. *Physiological Genomics*, **22**, 269-282. <http://dx.doi.org/10.1152/physiolgenomics.00229.2004>
- [40] Amores, A., Force, A., Yan, Y.L., Joly, L., Amemiya, C., Fritz, A., Ho, R.K., Langeland, J., Prince, V., Wang, Y.L., Westerfield, M., Ekker, M. and Postlethwait, J.H. (1998) Zebrafish Hox Clusters and Vertebrate Genome Evolution. *Science*, **282**, 1711-1714. <http://dx.doi.org/10.1126/science.282.5394.1711>
- [41] Postlethwait, J.H., Yan, Y.L., Gates, M.A., Horne, S., Amores, A., Brownlie, A., Donovan, A., Egan, E.S., Force, A., Gong, Z., Goutel, C., Fritz, A., Kelsh, R., Knapik, E., Liao, E., Paw, B., Ransom, D., Singer, A., Thomson, M., Abduljabbar, T.S., Yelick, P., Beier, D., Joly, J.S., Larhammar, D., Rosa, F., Westerfield, M., Zon, L.I., Johnson, S.L. and Talbot, W.S. (1998) Vertebrate Genome Evolution and the Zebrafish Gene Map. *Nature Genetics*, **18**, 345-349. <http://dx.doi.org/10.1038/ng0498-345>
- [42] Woods, I.G., Kelly, P.D., Chu, F., Ngo-Hazelett, P., Yan, Y.L., Huang, H., Postlethwait, J.H. and Talbot, W.S. (2000) A Comparative Map of the Zebrafish Genome. *Genome Research*, **10**, 1903-1914. <http://dx.doi.org/10.1101/gr.10.12.1903>
- [43] Taylor, J.S., Braasch, I., Frickey, T., Meyer, A. and Van de Peer, Y. (2003) Genome Duplication, a Trait Shared by 22000 Species of Ray-Finned Fish. *Genome Research*, **13**, 382-390. <http://dx.doi.org/10.1101/gr.640303>
- [44] Woods, I.G., Wilson, C., Friedlander, B., Chang, P., Reyes, D.K., Nix, R., Kelly, P.D., Chu, F., Postlethwait, J.H. and Talbot, W.S. (2005) The Zebrafish Gene Map Defines Ancestral Vertebrate Chromosomes. *Genome Research*, **15**, 1307-1314. <http://dx.doi.org/10.1101/gr.4134305>
- [45] Ruvinsky, A. and Watson, C. (2007) Intron Phase Patterns in Genes: Preservation and Evolutionary Changes. *The Open Evolution Journal*, **1**, 1-14. <http://dx.doi.org/10.2174/1874404400701010001>
- [46] Fedorov, A., Suboch, G., Bujakov, M. and Fedorova, L. (1992) Analysis of Nonuniformity in Intron Phase Distribution.

- Nucleic Acids Research*, **20**, 2553-2557. <http://dx.doi.org/10.1093/nar/20.10.2553>
- [47] Artamonova, I.I. and Gelfand, M.S. (2007) Comparative Genomics and Evolution of Alternative Splicing: The Pessimists' Science. *Chemical Reviews*, **107**, 3407-3430. <http://dx.doi.org/10.1021/cr068304c>
- [48] Ruvinsky, A. and Ward, W. (2006) A Gradient in the Distribution of Introns in Eukaryotic Genes. *Journal of Molecular Evolution*, **63**, 136-141. <http://dx.doi.org/10.1007/s00239-005-0261-6>
- [49] Fedorov, A., Roy, S., Fedorova, L. and Gilbert, W. (2003) Mystery of Intron Gain. *Genome Research*, **13**, 2236-2241. <http://dx.doi.org/10.1101/gr.1029803>
- [50] Roy, S.W. (2004) The Origin of Recent Introns: Transposons? *Genome Biology*, **5**, 251. <http://dx.doi.org/10.1186/gb-2004-5-12-251>
- [51] Ogino, K., Tsuneki, K. and Furuya, H. (2010) Unique Genome of Dicyemid Mesozoan: Highly Shortened Spliceosomal Introns in Conservative Exon/Intron Structure. *Gene*, **449**, 70-76. <http://dx.doi.org/10.1016/j.gene.2009.09.002>
- [52] Collins, L. and Penny, D. (2006) Investigating the Intron Recognition Mechanism in Eukaryotes. *Molecular Biology and Evolution*, **23**, 901-910. <http://dx.doi.org/10.1093/molbev/msj084>
- [53] Bo, X., Schoepfer, R. and Burnstock, G. (2000) Molecular Cloning and Characterization of a Novel ATP P2X Receptor Subtype from Embryonic Chick Skeletal Muscle. *The Journal of Biological Chemistry*, **275**, 14401-14407. <http://dx.doi.org/10.1074/jbc.275.19.14401>
- [54] Fountain, S.J., Cao, L., Young, M.T. and North, R.A. (2008) Permeation Properties of a P2X Receptor in the Green Algae *Ostreococcus tauri*. *The Journal of Biological Chemistry*, **283**, 15122-15126. <http://dx.doi.org/10.1074/jbc.M801512200>
- [55] Fountain, S.J., Parkinson, K., Young, M.T., Cao, L., Thompson, C.R. and North, R.A. (2007) An Intracellular P2X Receptor Required for Osmoregulation in *Dictyostelium discoideum*. *Nature*, **448**, 200-203. <http://dx.doi.org/10.1038/nature05926>
- [56] Dubyak, G.R. (2007) Go It Alone No More—P2X₇ Joins the Society of Heteromeric ATP-Gated Receptor Channels. *Molecular Pharmacology*, **72**, 1402-1405. <http://dx.doi.org/10.1124/mol.107.042077>
- [57] Bernier, L.P. (2012) Purinergic Regulation of Inflammasome Activation after Central Nervous System Injury. *The Journal of General Physiology*, **140**, 571-575. <http://dx.doi.org/10.1085/jgp.201210875>
- [58] Kaan, T.K., Yip, P.K., Patel, S., Davies, M., Marchand, F., Cockayne, D.A., Nunn, P.A., Dickenson, A.H., Ford, A.P., Zhong, Y., Malcangio, M. and McMahon, S.B. (2010) Systemic Blockade of P2X₃ and P2X_{2/3} Receptors Attenuates Bone Cancer Pain Behaviour in Rats. *Brain*, **133**, 2549-2564. <http://dx.doi.org/10.1093/brain/awq194>
- [59] Sperlagh, B. and Illes, P. (2014) P2X₇ Receptor: An Emerging Target in Central Nervous System Diseases. *Trends in Pharmacological Sciences*, **35**, 537-547. <http://dx.doi.org/10.1016/j.tips.2014.08.002>
- [60] Tsuchihara, T., Ogata, S., Nemoto, K., Okabayashi, T., Nakanishi, K., Kato, N., Morishita, R., Kaneda, Y., Uenoyama, M., Suzuki, S., Amako, M., Kawai, T. and Arino, H. (2009) Nonviral Retrograde Gene Transfer of Human Hepatocyte Growth Factor Improves Neuropathic Pain-Related Phenomena in Rats. *Molecular Therapy*, **17**, 42-50. <http://dx.doi.org/10.1038/mt.2008.214>

Supplementary

Table S1. Microsynteny of P2X subunit genes between mouse and human.

Mouse			Human	
	-2 Zzef1	zinc finger, ZZ-type with EF hand domain 1	Zzef1	2
	-1 Atp2a3	ATPase, Ca ⁺⁺ transporting, ubiquitous	Atp2a3	1
p2x1	P2rx1	purinergic receptor P2X, ligand-gated ion channel, 1	P2rx1	
	1 Camkk1	calcium/calmodulin-dependent protein kinase kinase 1, alpha	Camkk1	-1
	><		><	
	2 Itgae	integrin alpha E, epithelial-associated	Itgae	-2
p2x5	P2rx5	purinergic receptor P2X, ligand-gated ion channel, 5	P2rx5	
	4 Tmem93	transmembrane protein 93	Tmem93	-4
	5 Tax1bp3	Tax1 (human T-cell leukemia virus type I) binding protein 3	Tax1bp3	-5
	-2 Pxmp2	peroxisomal membrane protein 2	Pxmp2	2
	-1 Pole	polymerase (DNA directed), epsilon	Pole	1
p2x2	P2rx2	purinergic receptor P2X, ligand-gated ion channel, 2	P2rx2	
	><		><	
	1 Fbrsl1	fibrosin-like 1	Fbrsl1	-1
//				
	><		><	
p2x7	P2rx7	purinergic receptor P2X, ligand-gated ion channel, 7	P2rx7	
	><		><	
p2x4	P2rx4	purinergic receptor P2X, ligand-gated ion channel, 4	P2rx4	
	1 Camkk2	calcium/calmodulin-dependent protein kinase kinase 2, beta	Camkk2	1
	2 Anapc5	anaphase-promoting complex subunit 5	Anapc5	2
	-2 Prg2	proteoglycan 2, bone marrow	Prg2	2
	-1 Prg3	proteoglycan 3	Prg3	1
p2x3	P2rx3	purinergic receptor P2X, ligand-gated ion channel, 3	P2rx3	
	1 Ssrp1	structure specific recognition protein 1	Ssrp1	-1
	2 Tnks1bp1	tankyrase 1 binding protein 1	Tnks1bp1	-2
	-1 Thap7	THAP domain containing 7	Thap7	-1
	><		><	
p2x6	P2rx6	purinergic receptor P2X, ligand-gated ion channel, 1	P2rx6	
	1 Slc7a4	solute carrier family 7 (cationic amino acid transporter, γ + system), member 4	Slc7a4	1
	><		><	